The International Journal of Advanced Manufacturing Technology (2025) 140:1601–1624
https://doi.org/10.1007/s00170-025-16365-2

ORIGINAL ARTICLE

Manufacturing cost optimization of welded steel plate I-girders integrating hybrid construction and tapered geometry

Iván Negrin[1] · Moacir Kripka[2] · Víctor Yepes[1]

Received: 18 February 2025 / Accepted: 10 August 2025 / Published online: 26 August 2025

Abstract

Steel plate I-girders are widely used in the construction industry worldwide. While numerous studies have explored ways to enhance their benefits, few have simultaneously optimized both key mechanical components—geometry and material—to develop novel and more efficient typologies. This research employs metaheuristic optimization to explore alternatives to traditional I-girders, formulating optimization problems that integrate geometric and material variables in both transverse and longitudinal planes. The objective is to minimize manufacturing costs, accounting for material expenses and seven key production activities such as welding, cutting, or painting, while ensuring compliance with Eurocode 3 specifications. The results indicate that material selection dominates in short-span girders, whereas geometric optimization becomes more critical for longer spans. The most cost-effective solution identified is the transversely hybrid with variable section (THVS) girder, which features tapered geometry and hybrid material distribution between the flanges and the web. Based on these findings, practical design recommendations are provided, including optimal span-to-depth ratios, hybrid ratios, taper angles, and transition positions for variable cross-section configurations. A proposed design methodology incorporating these recommendations is validated through a case study, demonstrating that THVS elements can reduce costs by up to 70% compared to traditional designs. However, challenges related to material availability, fabrication complexity, and local buckling risks must be addressed to fully realize the potential of these designs. Future research should prioritize FEA and experimental testing to refine these typologies and update design codes to better account for tapered and hybrid girders.

Keywords Manufacturing cost · I-girder · Tapered girder · Hybrid steel girder · Structural optimization

1 Introduction

Improving the manufacturing process of large components is essential for enhancing efficiency, reducing costs, and ensuring precision in production. As demand for high-performance structural elements grows, advancements in manufacturing technology, such as improved welding techniques or refined machining strategies, play a crucial role in streamlining production while minimizing resource consumption and operational expenses [1].

Due to its high consumption of resources and environmental impact, one of the industries that most urgently needs to improve the sustainability of its manufacturing processes is the construction sector. A key structural component in construction is steel plate I-girders. Their manufacturing involves welding the separate plates to form the I-section structure. They are adopted as a cost-effective alternative to other elements, such as hot-rolled I-section beams [2]. Besides their outstanding load-bearing capacity, the custom fabrication process of plate girders affords the flexibility to create non-prismatic forms (i.e., tapered girders) in line with the variation of stresses along the girder span. This flexibility results in considerable material savings compared to prismatic sections (i.e., the same cross-section along the entire span), resulting in more economical designs [3]. Another advantage of this type of element is the possibility of implementing hybrid construction within the application framework of Modern Methods of Construction [4]. These structures are subjected to different stresses in their plates

✉ Iván Negrin
ianegdia@doctor.upv.es

[1] Institute of Concrete Science and Technology (ICITECH), Universitat Politècnica de València, Valencia 46022, Spain

[2] Civil Engineering Graduate Program, Federal University of Technology-Paraná, Via Do Conhecimento, Km 1, Pato Branco, Paraná 85503-390, Brazil

when bending. Modifying only the section geometry to cope with these stresses (e.g., thicker flanges) results in heavy and inefficient elements. Consequently, due to this difference in stress, a practical solution is to use different types of steel for the flanges and web, resulting in transversely hybrid steel elements [5]. Therefore, to increase these elements' structural efficiency and sustainability, the two components governing their mechanical configuration can be modified: geometry and material.

Mathematical optimization has become essential in addressing structural design challenges, especially as these problems increasingly involve complex input and output data. Optimization algorithms provide efficient solutions for such challenges. Several authors have investigated methods to optimize geometric configurations of steel structures [6]. For instance, Vinot et al. (2001) [7] utilized the sequential quadratic programming (SQP) method to optimize the shape and physical properties of thin-walled beam-like structures. More recently, Ozbasaran and Yilmaz (2018) [8] implemented the Big Bang-Big Crunch heuristic to optimize the shape of doubly symmetric I-beams with tapered flanges and web, resulting in practical insights into flange tapering and weight reduction. Martins et al. (2023) [9] utilized genetic algorithms to optimize the I-section steel girders' economic cost, achieving up to 30–35% material cost savings. Habashneh et al. (2024) [10] proposed a topology optimization method for steel beams under elevated temperatures, incorporating thermoelastic-plastic behavior and geometric imperfections through the BESO method. Their results highlight the interplay of thermal effects, imperfections, and nonlinear behaviors in robust design, and the generated openings mitigate heat transfer within the beams. Kim et al. (2024) [11] explored optimization strategies for roll-formed high-strength steel beams, addressing defects such as twisting, edge wrinkling, and cracking by introducing two innovative notch designs in coil sheets. Hwang et al. (2025) [12] investigated roller straightening techniques to improve the dimensional accuracy of H-beams using finite element modeling and optimization software.

Several studies extend optimization to more complex structures. For example, Kaveh et al. (2020) [13] tested metaheuristic algorithms to minimize the weight of 3D steel frames, demonstrating significant reductions with optimized non-prismatic elements. Elhegazy et al. (2023) [14] focused on direct construction cost optimization for various steel building systems, offering parametric studies based on building height. Hlal et al. (2024) [15] focused on enhancing the sustainability of composite road bridges by applying genetic algorithms to optimize multiple objectives, including weight, investment cost, life cycle cost, and environmental impact. Their work highlights the potential of stainless steel corrugated web girders in achieving efficient and sustainable structural designs. Chen and Li (2024) [16] introduced an intelligent optimization framework for high-rise steel structure construction, integrating a wireless sensor network with a multi-objective positioning algorithm to improve efficiency and safety. Their system enhances real-time monitoring and decision-making, reducing construction risks and optimizing resource allocation. Cucuzza et al. (2024a) [17] introduced an optimization framework for steel trusses using damped exponential constructability penalties. Their work emphasizes balancing structural complexity, standardization, and cost-effectiveness by minimizing member variety and overall structural expense. The methodology was validated using a trussed roof structure, demonstrating the efficiency of the Howe truss configuration. Similarly, Cucuzza et al. (2024b) [18] challenged traditional minimum-weight optimization approaches by focusing on reducing material waste through standardization. They employed a genetic algorithm integrated with the one-dimensional Bin Packing Problem, achieving a 40% waste reduction in steel trusses and 3D domes. Etaati et al. (2024) [19] tackled the challenges of large-scale truss frame optimization by proposing the Cooperative Coevolutionary Marine Predators Algorithm with a greedy search (CCMPA-GS). Their method employed a divide-and-conquer strategy to separately optimize shape and size variables, which was further refined using a context vector to ensure optimal cooperation among solutions. This approach outperformed 13 established metaheuristic algorithms in optimizing two large-scale truss structures, achieving 52% and 63.4% enhancements for 314-bar and 260-bar configurations, respectively. While presenting diverse and impactful methodologies, these studies exhibit limitations in problem formulation. Most focus primarily on weight optimization rather than economic or sustainability aspects, despite evidence that weight optimization does not always align with cost-efficiency, especially when manufacturing activities like welding and painting are included [20]. Additionally, many approaches focus solely on geometric variables, neglecting material optimization and practical applicability, thereby limiting their real-world impact.

Material is another component to be modified in the search for optimal mechanics, and multi-material approaches have shown great potential in enhancing structural efficiency [21]. As mentioned, welded I-section steel plate girders can benefit from hybrid construction. The hybrid ratio (R_h) in steel elements is related to the ratio between the yield strength of the flanges and web (f_{yf}/f_{yw}) [5]. Although this topic has been under development for several years, there are still some gaps in the research. Several works have focused on the structural behavior of these elements. For example, fatigue tests [22], web buckling resistance [23], failure mechanisms [24, 25], bending behavior [26–28], elastic–plastic flexural behavior considering the residual stress of welding [29], fire-resistance design [30], elements with web openings [31], or made by stainless steel [32]. However,

theoretical research on the advantages of this construction practice is yet to be completed, although some studies have revealed fascinating information. Transversely hybrid configurations have been found to improve the economic indices of homogeneous I-section girders by about 10% [33]. In a numerical study on the behavior of these elements as part of a mixed steel–concrete bridge, it is stated that hybrid solutions are the only ones that present good indicators in the three analyzed objectives (weight, economy, and environmental impact) [34]. These investigations have the limitation of not studying the exploitation of hybrid steel construction in depth. The study by Negrin et al. (2023) [20] explores this alternative to homogeneous construction in experiments examining this phenomenon thoroughly. The results show economic savings of up to 18% regarding homogeneous girders. The optimal solutions use configurations with R_h values close to 2. Therefore, it is concluded that hybridization benefits this type of constructive element. However, this study combines geometric and material optimization, but only in the transverse plane.

As previously noted, mathematical optimization has been widely applied to enhance the efficiency of I-section steel girders. However, most studies to date have focused on modifying only one aspect of mechanical resistance (either geometry or material) without simultaneously optimizing both. Furthermore, many adopt overly simplified objective functions, typically minimizing structural weight or material cost, without accounting for broader manufacturing considerations. A third key limitation is the neglect of material variation along both transverse and longitudinal planes, which precludes the exploration of advanced hybrid configurations. Therefore, this study aims to overcome these limitations by using metaheuristic optimization as the design tool, formulating an optimization problem that explores the optimal mechanical design of welded steel plate I-girders in depth. Most importantly, the optimization framework is centered on a manufacturing cost-based objective function that includes not only material use but also key production activities (such as welding, painting, cutting, or transportation), thereby bridging structural design with the realities of manufacturing planning and resource efficiency. The constraints used are based on Eurocode 3, ensuring alignment with current design standards. Once all the alternatives have been explored, the most efficient ones are highlighted, and a series of design recommendations are stated. Finally, a simple and novel design methodology is proposed based on the recommendations formulated.

The structure of the paper is as follows: Sect. 2 summarizes the methodology employed, highlighting the concept of optimal mechanical configuration, its formulation as an optimization problem, and the strategy to solve it. Section 3 is intended to expose and discuss the results. Based on the results and limitations of the study, an analysis of future research lines is made. Finally, the conclusions of the study are drawn.

2 Methodology

This study employs a welded steel plate girder as its fundamental structural component. The structure is simply supported and subjected to a distributed load. In Fig. 1a, note

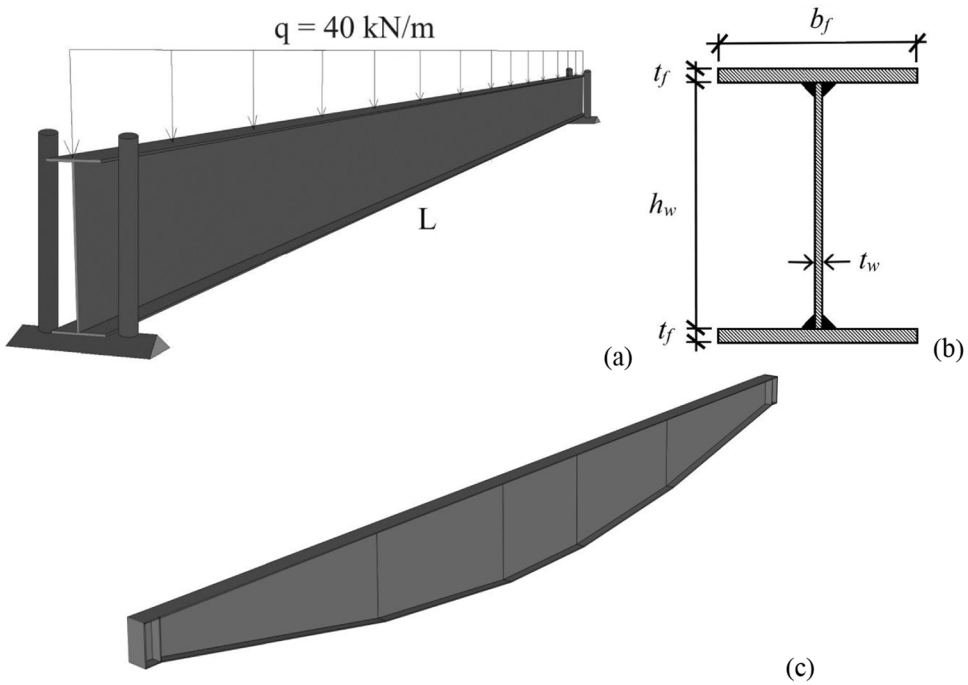

Fig. 1 **a** 3D basic case study; **b** cross-section with some geometric variables [20]; **c** variable section girder (tapered girder) with 4 transition points (TPs)

the depiction of fork-type supports, highlighting the restriction of rotational movement around the longitudinal axis. The distributed load assumption is derived from supposing the girder is a joist supporting a concrete slab or similar structure. It is crucial to recognize that even in supporting a slab (or similar structure), the girder lacks adequate transverse stiffness to dismiss lateral-torsional buckling. Consequently, the study addresses the reduction in bending resistance resulting from this phenomenon.

The joints between the plates are made by welding. Welding is also used to join the different sections in longitudinally hybrid configurations. It should be noted that although welding different types of steel does not pose practical problems, it is essential to have a good knowledge of the appropriate electrodes. The standards governing steel components establish criteria for using suitable electrodes, depending on the quality of the steel used. It is advisable to use electrodes that match the strength of the web, thus ensuring the strength of the web-flange weld [35]. As a simplification, residual stresses in welded joints are neglected.

The girder span is varied to obtain the three case studies. Three 6, 14, and 20 m specimens simulate elements belonging to different structures. For example, the shorter girder may be part of a frame building, while the longer one may be part of a bridge. In agreement with the previous study [20], the load value q is 40 kN/m. Note that this value represents an increased load state established for the ultimate limit state. A 75% reduction of the load value is considered to analyze the serviceability limit state. This experiment aims to study the different combinations of optimal mechanics for small and medium-span steel I girders.

2.1 Optimal mechanical configuration in steel I girders

Both the geometry and the material can be varied to regulate the mechanical resistance of a structural element. The search for the optimal design of I-section steel girders is an exciting problem due to the number of variables that can be involved in a single element. If we were to make a spectrum of optimal mechanics in these elements (see Fig. 2), we would have purely geometrical optimization at one extreme. On the other hand, we would have purely material optimization.

Starting at the left extreme of the spectrum is purely geometric optimization. The most complete case of geometry optimization (leaving the material fixed) that could be found is that of the optimized homogeneous girder with variable section (HoVS). The different cross-sections are optimized in the longitudinal plane to optimally comply with the constraints associated with the internal forces varying along the element. If we move to the right, it starts to "mix" both mechanical resistance components of the structure. The first case would be a transversely hybrid variable section (THVS) girder. In this instance, there is also a powerful geometrical optimization component, but the material of both plates (flanges and web) is differentiated and optimized.

In the middle of the spectrum, we have what is theoretically the most complete option since, in this situation, both components are combined as freely as possible, varying over the entire length of the element (transverse and longitudinally hybrid girders with variable section, TLHVS). However, this solution may be a bit misleading. Solutions can be complex if an optimization algorithm can modify

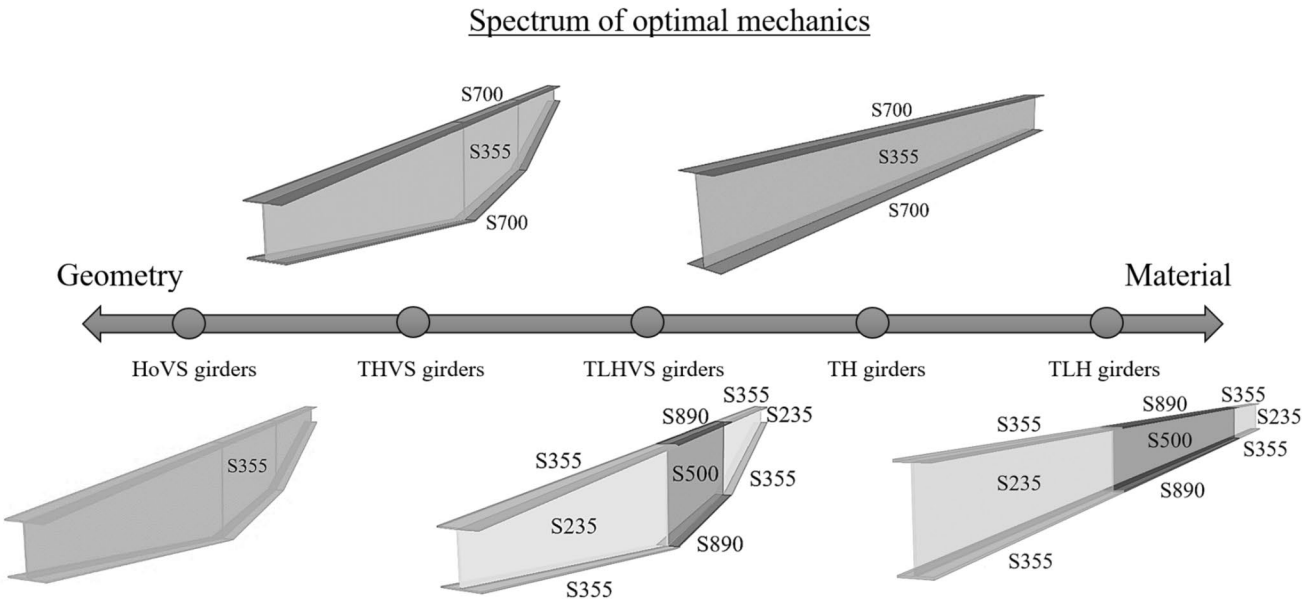

Fig. 2 Location of general typologies within the spectrum of optimal mechanics in I-section steel girders

geometrical and material parameters along the element. For example, elements with "strange" geometrical shapes can be obtained that could be prone to certain local phenomena. The same applies to the material, where "optimal" configurations can be complex to build. Another problem this type of typology could generate is the need to establish additional joints due to the change of material in the longitudinal direction.

A further step to the right is moving away from the geometry part of the spectrum and towards the material part. Transversely hybrid (TH) girders are the same case as THVS but with constant cross-section. In this case, a single optimal geometrical configuration is sought, and the material is optimized in the element plates along its entire length [20]. Note how this typology is more to the right (towards the material configuration) than the previous case (TLHVS girders), even though the latter develops a more substantial component in this field than the former. Nevertheless, the TH girders are simultaneously farther apart from the optimal geometrical configuration than the TLHVS. Moreover, the latter are located in the middle of the spectrum to reflect the equal combination of both parameters.

Finally, the transverse and longitudinal hybrid (TLH) girders are on the far right. Finding this last case in a pure state is rare in structural optimization. This type of element is somehow associated with geometric optimization. Selecting a profile from a catalog (with a preset geometric configuration) and optimizing the material configuration would represent this approach. However, the logical methodology is to start from dimensions previously established by some criteria. The opposite extreme can also mix the optimization of both components since, in HoVS girders, the material type of the whole element could also be optimized. It is important to point out that this research represents a leap in quality to the previous study since, in addition to the TH configuration, four other novel typologies are investigated by varying material and geometry in the transversal plane, but also in the longitudinal direction.

2.2 Optimal mechanics problem formulation

In this study, the different optimization problems are formulated in a way that allows the optimization algorithm to explore and develop the typologies located in the optimal mechanic's spectrum represented in Fig. 2. Figure 3 shows the different approaches adopted in the design and how they relate to the typologies located in this spectrum. The essential formulation is based on the previous study [20], but the implementation of longitudinal optimization results in a new set of variables. It also causes the constraints to be evaluated to a greater or lesser extent for each case. The optimization objective is the same for all problems. The only variation is

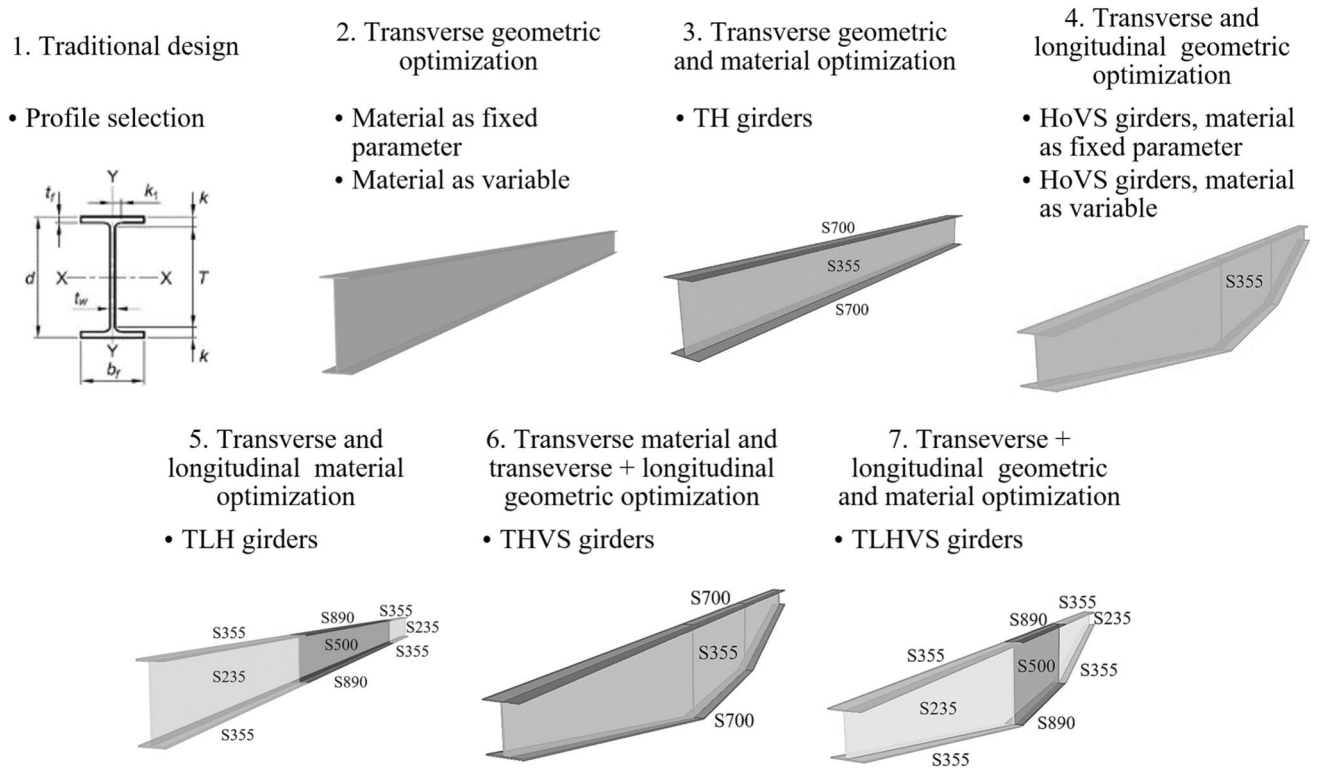

Fig. 3 Approaches adopted in the design and corresponding typologies to be studied

incorporating the additional costs of the joints required for elements with longitudinal hybridization.

2.2.1 Variables

It is necessary to establish that there are three groups of variables. The most basic is related to the geometry of the central cross-section (Fig. 1b). In this group, there are four variables. The variables related to the width of the plates (h_w, b_f) are formed into a vector B consisting of 91 values. The limits of the range of motion of the variable h_w are different depending on the case study. It is so that the optimization algorithm can explore the optimal mechanical configurations (geometry + material). That is, depending on, e.g., the *to point out that* length of the element, the lower and upper bounds are modified so that the vector B has 91 values, and the element plates can reach their optimal width. For the 6 m elements, the vector B varies from 100 to 1000 mm, while for the 20 m elements, the limits would be from 2000 to 2900. If, in any case, there is an optimal value near the limits, these are readjusted so that this value would be in the center of the interval. The variable b_f always has limits (100, 1000). The variables associated with the plate thicknesses (t_w, t_f) have a solution space as shown in the vector T of Eq. 1 (19 values).

$$T = \{5, 6, 8, 10, 12, 14, 15, 16, 18, 20, 22, 25, 30, 35, 40, 50, 60, 80, 100\}(mm) \quad (1)$$

The other group of variables corresponds to the configuration of the material in the plates (f_{yw}, f_{yf}). Eleven types of steels are included in the formulation, with the restriction that the yield strength of the flanges f_{yf} does not exceed twice that of the web f_{yw} [36]. The vector M, shown in Eq. 2, represents the eleven possible alternatives. It should be noted that all these steel types are assumed to be available, as it opens up the possibility of improving the implementation of hybrid configurations. These ranges of geometrical variables, as well as the selection of steel types (material variables), have been established in correspondence with previous studies.

$$M = \{S235, S275, S355, S420, S450, S500, S550, S600, S700, S890, S960\} \quad (2)$$

The final group of variables is associated with the positioning of transitions. Remember that these can be related to geometry or material components. So far, the variables mentioned are discrete. The same happens with this group of variables. The transition points (TPs) are placed at values multiples of 5 cm (50, 100, 150, …, L/2 mm) starting from the element's extreme to give it a real approach. It ensures that its configuration is constructively coherent. Thus, each transition point can be placed at *[(L/2)/50]−2* number of positions (L in mm). For example, for the 6 m girder, the variables related to this aspect can take 58 values; for the 14 m girder, a total of 138, and further. Note that since the element is symmetrical, a variable is set for each of the two diametrically opposed TPs. For example, in Fig. 1c configuration, four TPs (two for each half of the element) move symmetrically, assigning two optimization variables. One of these variables is formulated for the configuration with two TPs. For the configuration with six, three are formulated.

In summary, all problems are formulated with four essential geometric variables related to the cross-section. One or two variables related to steel grade are added: one when optimizing the material of a homogeneous element (approach two or four in Fig. 3), and two when dealing with a transversely hybrid element (approach three and six in Fig. 3). However, when problems are formulated to explore longitudinally variable elements, other variables such as those regulating the position of the transition appear. If the geometry is varied, new variables are introduced for the h_w value of the new sections (t_w, b_f, and t_f are kept the same as in the central section). If the material is varied, two values of f_{yf} and f_{yw} are introduced for each new element's span. For example, in the typology shown in the fifth approach in Fig. 3, no additional variables are introduced concerning geometry. However, two are introduced to regulate the type of steel in the flanges and web of the extreme sections. The most complex case would be the 20 m TLHVS girder (seventh approach in Fig. 3) with six transitions. This case would be formulated with the four essential geometric variables for the central section and two to regulate this section's material. From here, the additional ones are incorporated: three to regulate the position of the TPs, three to regulate the width of the web of the other three sections, and six for the type of material in the plates of the other three spans (three for each half of the element) formed with the transitions.

The vector $\boldsymbol{X}$ (Eq. 3) represents the above configuration of variables. Note how, in addition to the six essential variables, four groups with subscripts i are incorporated to represent the position of the transitions (x), the h_w values of the other sections, and the configuration of the steel in the different sections formed by establishing transitions (if the element is longitudinally hybrid, approach five and seven in Fig. 3).

$$\boldsymbol{X} = \left\{ h_w, t_w, b_f, t_f, f_{yw}, f_{yf}, x_i, h_{w_i}, f_{yw\_i}, f_{yf\_i} \right\} \quad (3)$$

2.2.2 Objective function

The objective function developed in this study represents the total manufacturing cost of the steel girder, going far beyond traditional weight-based metrics. It includes not only material cost, but also a comprehensive set of seven fabrication-related activities: erecting, painting, welding, blasting,

cutting, sawing, and transportation. This formulation reflects the real-world sequence of manufacturing operations and is specifically developed for single-piece production, rather than batch-sized fabrication. The cost function is defined in Eq. 4a. Here, both productive and non-productive times are considered when calculating the costs of individual activities, following the methodology outlined in [33]. By incorporating these aspects, the model offers a more accurate reflection of real-world fabrication processes and production workflows, and positions the optimization framework at the intersection of design innovation and manufacturing practicality. This dual focus provides structural efficiency and actionable insights for manufacturers seeking to improve production planning and cost control.

$$\begin{aligned} &M_B(X) = C_M(X) + C_E(X) + C_P(X) + C_W(X) + C_B(X) \\ &+C_C(X) + C_S(X) + C_T(X)(\in) \quad (4a) \\ &M(X) = M_B(X) + C_J(X)(\in) \quad (4b) \end{aligned} \tag{4}$$

Unlike previous research, the introduction of longitudinal hybridization requires additional joints in the girder construction. Equation 4a illustrates the cost of joining the three plates to form the basic element shown in Fig. 1a. However, the element sections must also be joined longitudinally to establish material changes in the longitudinal direction. Thus, the objective function $M(\boldsymbol{X})$ is formulated as presented in Eq. 4b. If no additional joints need to be implemented, the objective function would be Eq. 4a. In Eq. 4b, the cost of joints ($C_J(\boldsymbol{X})$) is determined analogously to the calculation for plate joining shown below. It implies additional costs for cutting, sawing, blasting, and welding. The importance of this additional cost lies in determining whether the assumed cost savings from using different materials over the entire length of the element are substantial enough to justify the application of the material transition. Note that it is also necessary to make additional joints in the lower flange plates on the tapered girders.

For material costing, the coefficient K_M is introduced to represent the relative costs of different steel types compared to a baseline material. Since steel prices can vary significantly, a base cost of 0.7 €/kg is assumed for S355 steel, with K_M values expressing the cost of other steel grades relative to this reference. For instance, S420 steel is 1.07 times the cost of S355 steel. These values are derived from [33], where cost penalties for various steel grades are systematically incorporated, as shown in Table 1. The cost data was established in collaboration with experts in the steel manufacturing industry [33].

For steel grades not explicitly covered in the referenced study, a linear interpolation method is used to estimate their coefficients. The same interpolation approach is applied to other coefficients listed in Table 1. The material cost

Table 1 Cost parameters according to steel grades

Steel grade	K_M	C_w	Welding (K_W)	Sawing (K_s)
S235	0.88	0.34	0.79	0.88
S275	0.92	0.41	0.86	0.92
S355	1.00	0.55	1.00	1.00
S420	1.07	0.66	1.11	1.07
S450	1.10	0.71	1.16	1.10
S500	1.15	0.80	1.25	1.15
S550	1.19	0.80	1.31	1.19
S600	1.23	0.81	1.38	1.23
S700	1.30	0.82	1.50	1.30
S890	1.44	0.84	1.74	1.44
S960	1.50	0.84	1.83	1.50

$C_M(\boldsymbol{X})$ is formulated in Eq. 5 where K_M values are separately defined for the flanges (K_{Mf}) and the web (K_{Mw}) to accommodate hybrid configurations. The term ρ represents the steel density (7.85·10-6 kg/mm3).

$$\mathrm{C_M(X)} = 0.7\rho L(\mathrm{K_{Mf}}2\mathrm{b_f t_f} + \mathrm{K_{Mw}h_w t_w})(\in) \tag{5}$$

Note that several of these activities are also related to the element's life cycle. For example, transportation or erecting costs are related to the construction stage. On the other hand, activities such as painting are associated (in addition to the manufacturing stage) with the maintenance stage. Finally, the end-of-life stage is also associated with costs such as erecting (disassembly in this case) and transportation, considering that the element will be recycled or reused.

Regarding the additional activities, the erecting cost $C_E(\boldsymbol{X})$ is obtained as in Eq. 6a. It is calculated based on a labor cost C_{LE} of 3.10 €/min, a crane cost C_{EqE} of 1.35 €/min, and a utilization factor u_E of 0.36. The time required to erect the girder $T_E(\boldsymbol{X})$ is determined in Eq. 6b, considering a lifting distance L_S of 15,000 mm and six bolts per joint ($n_b = 6$). Since the number of bolts per joint and the crane capacity remain constant, the erection cost depends only on the girder length.

$$\begin{aligned} &C_E(X) = T_E \frac{C_{LE}+C_{EqE}}{u_E}(\in) \quad (6a) \\ &T_E(X) = \frac{L}{30000} + \frac{L_S}{27000} + 2\left(0.5n_b - 0.42\right) + \frac{L_S}{36000}(\mathrm{min}) \quad (6b) \end{aligned} \tag{6}$$

The painting cost $C_P(\boldsymbol{X})$ follows the alkyd painting system proposed by Haapio (2012) [37] and is determined using Eq. 7a. The painted surface area per unit length $A_P(\boldsymbol{X})$ considers the width and thickness of the flanges, the height of the web, and excludes the top surface of the upper flange due to coverage by the upper structure (see Eq. 7b). The drying process is incorporated into the total painting cost calculation.

$$C_P(X) = 4.17 \bullet 10^{-6} L A_P(X) + 0.36 L b_f \bullet 1 \bullet 10^{-6} (\in) \quad (7a)$$

$$A_P(X) = 3b_f + 4t_f + 2h_w - 2t_w (mm^2/mm) \quad (7b)$$

(7)

The welding cost $C_W(\boldsymbol{X})$ assumes an automatic submerged arc welding process and is expressed in Eq. 8a. The base welding cost C_{CBW} and energy cost C_{EnBW} are 1.36 €/min and 0.08 €/min, respectively, with a non-productive time T_{NBW} of 6.25 min. The productive welding time $T_{PBW}(\boldsymbol{X})$ is given in Eq. 8b and depends on the welded length L_w (mm) and a thickness factor C_w that varies with the steel grade of the web. These thickness factors are derived from previous studies and account for total weld resistance. For instance, for S355, the weld thickness is $a_w = 0.55 t_w$, and the like. Since the base expression represents the welding of a single flange to the web, the productive time $T_{PBW}(\boldsymbol{X})$ is doubled to obtain the total welding time for both flanges. For longitudinally variable configurations (in geometry or material), the productive time is adjusted according to the number of additional plates to be welded. To reflect the increased cost of welding high-strength steels, the correction factor K_W is introduced, which adjusts the costs according to the highest steel grade used in the plates being welded (see Table 1).

$$C_W(X) = 2K_W[1.36\left(T_{NBW} + T_{PBW}(X)\right) + T_{PBW}(X) \left(C_{CBW} + C_{EnBW}\right)](\in) \quad (8a)$$

$$T_{PBW}(X) = \frac{7.85 \bullet 10^{-6} L_w a_w^2}{14} = \frac{7.85 \bullet 10^{-6} L_w C_w^2 t_w^2}{14} (\text{min}) \quad (8b)$$

(8)

Blasting and cutting costs do not vary with steel quality. The blasting cost $C_B(\boldsymbol{X})$ depends on the number of plates and their length L (mm) before welding, as expressed in Eq. 9.

$$\mathrm{C_B(X)} = 3 \bullet 3.64 \bullet 10^{-4} \mathrm{L} (\in) \quad (9)$$

The cutting cost $C_C(\boldsymbol{X})$ is given in Eq. 10a, with a non-productive time T_{NCu} of 3.0 min. Plasma cutting is used for plate thicknesses up to 30 mm, while flame cutting is applied to thicker plates. The productive time for plasma cutting T_{PCu} (Eq. 10b) depends on the plate thickness t (mm), with consumable and energy costs (C_{CCu} and C_{EnCu}) of 0.38 €/min and 0.12 €/min, respectively. The total cut length L_{Cu} includes both the flanges and the web (in mm). For flame cutting, the productive time T_{PCu} and consumable costs C_{CCu} are calculated using Eqs. 10c and 10d, respectively. Energy consumption is considered negligible. The cutting cost for the flange plates is obtained by multiplying Eq. 10a by two. As in welding, configurations that vary in the longitudinal direction require certain adjustments.

$$\mathrm{C_C(X)} = 1.32\left(\mathrm{T_{NCu}} + \mathrm{T_{PCu}(X)}\right) + \mathrm{T_{PCu}(X)}\left(\mathrm{C_{CCu}(X)} + \mathrm{C_{EnCu}}\right) (\in) \quad (10a)$$

$$\mathrm{T_{PCu}(X)} = \frac{\mathrm{L_{Cu}(X)}}{8.92t^2 - 486.87t + 8115.8} (\text{min}) \quad (10b)$$

$$\mathrm{T_{PCu}(X)} = \frac{\mathrm{L_{Cu}(X)}}{-4.19t + 658.67} (\text{min}) \quad (10c)$$

$$\mathrm{C_{CCu}(X)} = 0.22 + 4.18\left(1 \cdot 10^{-5} t^2 + 0.001t + 0.0224\right) \quad (\in / \text{min}) \quad (10d)$$

(10)

The sawing cost $C_S(\boldsymbol{X})$ is determined using Eq. 11a. The non-productive time for sawing is given by $T_{NS} = 4.5 + L/20000$ (min). The energy cost is $C_{EnS} = 0.02$ €/min. The productive time T_{PS} depends on the position of the cross-section during sawing. It is assumed that the girder is laid on its side, meaning the flanges are sawn vertically and the web horizontally. To account for variations in steel grades, cost factors $K_{S,f}$ and $K_{S,w}$ are introduced into the production time calculation, as shown in Eq. 11b. The cost of consumables C_{CS}, which includes the wear of saw blades, is determined using Eq. 11c. This calculation considers the saw blade price p_{SB} (100 €) and a thickness-dependent parameter F_{sp}, as shown in Table 2. The feeding speed S of the saw depends on the plate thickness, with values also provided in Table 2. The geometric properties of the section (b_f, t_f, h_w, t_w) are illustrated in Fig. 1.

$$\mathrm{C_S(X)} = 1.20\left(\mathrm{T_{NS}} + 2\mathrm{T_{PS}(X)}\right) + 2\mathrm{T_{PS}(X)}\left(\mathrm{C_{CS}(X)} + \mathrm{C_{EnS}}\right) (\in) \quad (11a)$$

$$\mathrm{T_{PS}(X)} = \mathrm{K_{S,f}} \frac{\mathrm{b_f}}{0.9\mathrm{St_f}} + \mathrm{K_{S,w}} \frac{\mathrm{h_w t_w}}{8800} (\text{min}) \quad (11b)$$

$$\mathrm{C_{CS}(X)} = \mathrm{p_{SB}} \frac{2\left(\mathrm{b_f t_f}\right) + \left(\mathrm{h_w t_w}\right)}{11.88 \bullet 10^6 \mathrm{F_{sp}}\left(\mathrm{t_f}\right)\mathrm{T_{PS}(X)}} (\in / \text{min}) \quad (11c)$$

(11)

Finally, the transportation cost $C_T(\boldsymbol{X})$ is determined by whether the weight-to-volume ratio of the girder exceeds a predefined threshold. If the ratio is below this limit, the cost is calculated based on the beam's volume; otherwise, it is based on its weight (see Eq. 12). The volume is expressed in m^3, and the weight is expressed in kilograms. The assumed transportation distance from the workshop to the construction site d_{ws} is 200 km.

$$C_T(X) = \begin{cases} V(X)\left(0.0106 d_{ws} + 1.2729\right), if \frac{W(X)}{V(X)} \le 264 \\ W(X)\left(4 \bullet 10^{-5} d_{ws} + 4.8 \bullet 10^{-3}\right), otherwise \end{cases} (\in) \quad (12)$$

2.2.3 Constraints

Optimization problems are governed by constraints that ensure correct design. These are based on Eurocode 3 [36, 38]. The proposed design methodology is derived from [33]

Table 2 Saw feeding rate S and parameter F_{sp} according to Mela and Heinisuo (2014) [33]

Plate thickness (mm)	S (mm/min)	F_{sp}
5	120	0.40
6–10	100	0.45
11–15	90	0.50
16–20	80	0.55
21–25	70	0.60
26–30	60	0.65
31–35	40	0.70
≥ 36	50	0.80

and [35], with adjustments proposed in [20]. Two constraints already mentioned consist of limiting the yield strength of the flange steel so that it does not exceed twice that of the web. The other one concerns the transition points, where the possibility of these points moving all over the middle of the element makes it necessary to restrict their positions to be correct. The first transition point must be placed before the second, the second before the third, and the like.

Another important set of constraints relates to compliance with strength and serviceability limit states. For longitudinally homogeneous girders, the flexural strength checks consider the highest moment at the center of the span, ensuring the overall strength of the proposed cross-section. The shear checks focus on the highest values at the supports and other critical points. Longitudinally variable configurations (either material or geometry), on the other hand, present several cross-sections. Therefore, they require additional checks. In the case of bending moment, both the extremes of each new span and a discrete number of intermediate points are checked since the cross-section does vary linearly, but the moment does not. The bending-shear interaction is ruled out because the element is simply supported, so this phenomenon does not significantly affect the girder. The most critical aspects are summarized below. Consult the cited references for further details.

The bending resistance constraint is summarized in Eq. 13. Remember that in longitudinally variable configurations, several cross-sections are checked. Due to its symmetry, the analysis is conducted on just one half of the girder. In this context, $M_{Rk}(\boldsymbol{X})$ denotes the bending resistance of the section, while M_{Ed} represents the maximum acting bending moment. For the central configuration, M_{Ed} is $q_T L^2/8$. To check other sections, the bending moment equation for half of the element is used. It is worth noting that the subscript T is appended to the distributed load term q, indicating the total load, which includes the element's self-weight.

$$M_{Rk}(\boldsymbol{X}) \geq M_{Ed} \tag{13}$$

Considering that the methodology proposed by Mela and Heinisuo (2014) [33] is cumbersome when the top flange or web belongs to a class higher than 2, an approach proposed by Veljkovic and Johansson (2004) [35] is used. This procedure can be entirely found in [20].

The reduction factor for lateral buckling can be considered as for homogeneous girders. This factor affects the cross-section bending resistance M_{Rk}. The strength reduction process is detailed in Eurocode 3–1-1 ([38], Sect. 6.3.2). According to the alternative procedure proposed by [35], the slenderness parameter (λ_{LT}) can be obtained from Eq. 14. Here, M_{cr} represents the critical bending moment based on elastic stability theory, calculated from the gross properties of the cross-section. This parameter is essential to obtain the global reduction factor according to Eurocode 3–1-1.

$$\lambda_{LT}(\boldsymbol{X}) = \sqrt{M_{Rk}(\boldsymbol{X})/M_{cr}} \tag{14}$$

The shear resistance constraint is outlined in Eq. 15. The maximum shear at the supports is denoted by $V_{Ed} = q_T L/2$. $V_{c,Rd}(\boldsymbol{X})$ represents the plastic shear resistance obtained in accordance with Eurocode 3–1-5 ([36], Sect. 5). As per Eurocode 3–1-1 ([38], Clause 5.1(2)), the shear buckling must be considered if the ratio of h_w/t_w exceeds $72\varepsilon/\eta$. Subsequently, transverse stiffeners must be installed at the element's supports, as stated in Clause 5.1(2) of [38] and Sect. 9.3 of [36].

$$V_{c,Rd}(\boldsymbol{X}) \geq V_{Ed} \tag{15}$$

In the case of type 2 tapered girders (the ones analyzed in this study), the effect of the tension field is ignored since it has been demonstrated that in this case, increasing the taper angle increases the resistance to elastic shear buckling. Refer to [2, 3] to check typologies 1 and 2 associated with this phenomenon.

On the other hand, the h_w/t_w ratio must satisfy the criterion detailed in Eq. 16, as specified in Clause 8(1) of [38], to prevent the compression flange buckling in the web plane. Here, E represents the modulus of elasticity of the steel (210 000 MPa), A_{fc} stands for the effective cross-sectional area of the compression flange, and the coefficient k is set at 0.40 for plastic moment resistance or 0.55 for elastic moment resistance.

$$\frac{h_w}{t_w} \leq k\frac{E}{f_{yf}}\sqrt{\frac{h_w t_w}{A_{fc}}} \tag{16}$$

In the case of stiffness, Eq. 17a represents this constraint. Here, $\overline{u}$ is the maximum allowable displacement, which is established as $L/400$. The maximum displacement is obtained from Eq. 17b, where q_{SLS} is the serviceability limit state load (in N/mm), considered $0.75q$, and I_y is the inertia of the cross-section regarding the bending axis (in mm^4).

$$u_{max}(X) \leq \overline{u} \tag{17a}$$

$$u_{max}(X) = \frac{5}{384}\frac{q_{SLS}\,L^4}{E I_y\,(X)} \tag{17b}$$

For tapered girders, the value of I_y used in Eq. 17 b is obtained by calculating a weighted average inertia using the different sections as a function of the length of the spans to which they belong. The procedure has been validated using finite element software.

2.2.4 Mathematical formulation of the problem

In conclusion, the problem is formulated with discrete variables, the number of which varies according to the case study. Equation 18 provides the general mathematical representation of the problem. Additional constraints are represented, such as those governing the position of the transition points ($x_i < x_{i+1}$). This requirement ensures that the transition points are ordered, i.e., no x_i exceeds the next x_{i+1}. This condition applies to problems in configurations with more than two TPs. In configurations with two TPs, the position of the point oscillates between 0 and $L/2$ without reaching either of the two extreme values.

$$\begin{aligned} &\min\ M(X) \\ \text{Such that } &M_{Ed} \le M_{Rk}(\boldsymbol{X}) \\ &V_{Ed} \le V_{c,Rd}(\boldsymbol{X}) \\ &\frac{\mathrm{h_w}}{\mathrm{t_w}} \le \mathrm{k}\frac{\mathrm{E}}{\mathrm{f_{yf}}}\sqrt{\frac{\mathrm{h_w t_w}}{\mathrm{A_{fC}}}} \\ &u_{max}(X) \le \overline{u} \\ &f_{yf} \le 2 f_{yw} \\ &x_i < x_{i+1} \\ &b_f, h_w \in \boldsymbol{B} \\ &t_f, t_w \in \boldsymbol{T} \\ &f_{yf}, f_{yw} \in \boldsymbol{M} \end{aligned} \tag{18}$$

It should be noted that these problems are nonlinear optimization. In addition, there are some discontinuities in the constraint functions, such as in the bending strength constraint in the zones where the cross-section class changes. Therefore, the mathematical properties of the constraints make it challenging to find the global optimum. It rules out the use of nonlinear discrete optimization methods [20]. Here is where heuristics play a decisive role due to their flexibility and efficiency in solving this type of problem.

2.3 Solution of the optimization problem

To provide a heuristic solution to the problem, a method that has demonstrated excellent effectiveness in discrete optimization has been selected [39]. It is called biogeography-based optimization (BBO), which was proposed by Simon (2008) [40]. Its superiority over other heuristics in these conditions is due to the recombination and mutation operator used [41]. While other similar heuristics take two solutions to generate a new one (the general procedure is executed from solution to solution), BBO operates at a variable level, allowing the formation of a new solution from multiple preceding ones rather than just two. Furthermore, both the combination and mutation operators influence the variables, generating new solutions within a single operation. Unlike mutating the entire solution simultaneously, mutation occurs at the variable level, potentially impacting a solution multiple times. For further insights into the functioning of this method, refer to the provided bibliography.

Parameter tuning processes are performed for each group of problems to ensure maximum performance. In conjunction with the experience gained from previous work, problems are solved efficiently. However, more than the basic method is needed to achieve stability in the results of some case studies. That is why a strategy called biogeography-based sequential optimization with evolving limits (BBSOEL) is proposed. It consists of dividing the global search into several searches, while the limits shrink and evolve according to the best solution partially found. It allows for the search to be refined while reducing the solution space.

BBSOEL starts with a global search of the entire solution space. Once completed, four local searches with reduced bounds are performed. For each search, the parameters are tuned (see Fig. 4). The range of movement of each variable is reduced to 25%. For example, the variables associated with the section dimensions that can initially take 91 values are reduced to 23, and so on. The new interval is created from the best value found. For example, if that phase's "optimal" value is 45, the new interval would be set to (34, 56). If in the other phase (with the solution space reduced, which facilitates the search), the optimal value is set to 37, the limits evolve to (26, 48), and so on. Note that if the "optimal" value is close to the global limits, it proceeds so that the interval remains 23 values. For example, if 5 is obtained as the value of the best solution for that phase, the new limits would be (1, 23). For local searches, the population size parameter is reduced significantly (see Fig. 4) since another feature of BBO is its good performance with small population sizes.

The general metaheuristic procedure consists of running optimization processes until it is ensured that the optimum found is or is very close to the global optimum, according to the methodology based on the extreme value proposed by Paya-Zaforteza et al. (2010) [42]. It is necessary to highlight that in most problems, this global optimum is found simply, while in some, the search becomes more difficult. It is here where BBSOEL shows its superiority over the basic method.

Figure 4 shows two average performance curves (average fitness as a function of the iteration number) for the traditional procedure and the BBSOEL. After 25,000 function evaluations, it is appreciated how the proposed method (unlike the basic one, which stagnates on the best solution found so far) can reorganize the search and keep improving the solutions. In this representation, it appears that the improvement is not substantial. However, it should be

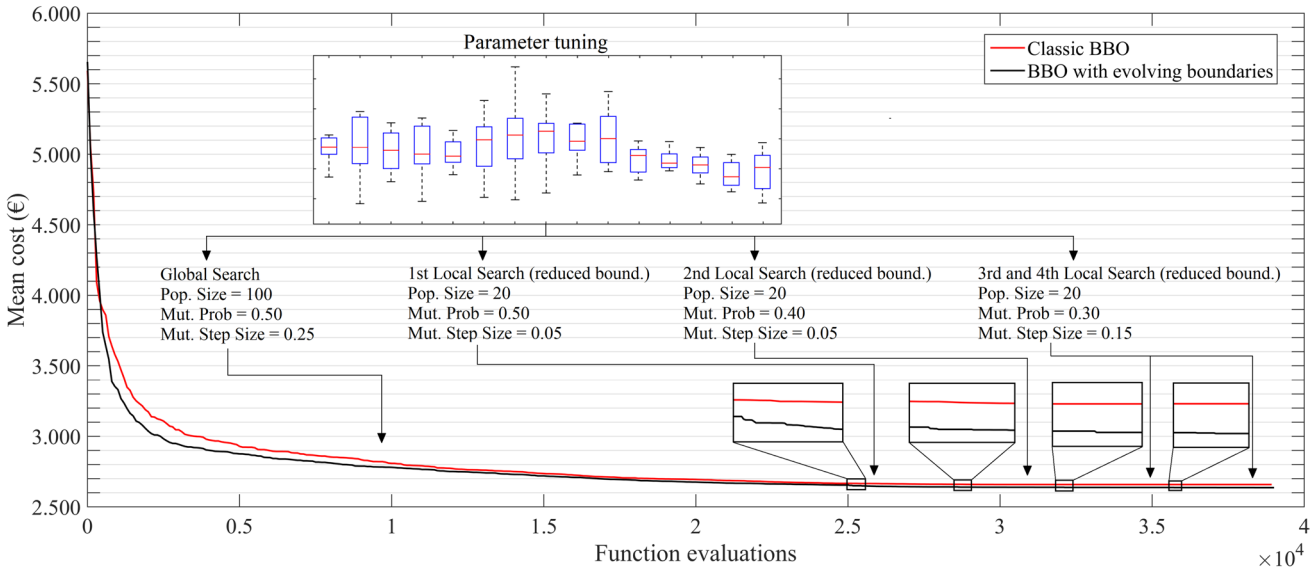

Fig. 4 Average performance curves of 30 optimization processes applied to the case study of the TLHVS girder of $L = 20$ m with 6 TPs

remembered that this curve is the average representation of 30 optimization procedures. Moreover, since function evaluations are not computationally costly processes, the objective is to find the global optimum, which the proposed method guarantees more than the basic one.

3 Results and discussion

For evaluating and discussing the results, each element is analyzed separately, exposing the main characteristics of each typology according to the design approach implemented. Subsequently, a summary of the main properties of each structure is made, and practical design recommendations are extracted. These are applied to a different case study, and the results are compared.

3.1 Girder of 6 m

This is a short-length element, so its use is intended primarily for buildings. Table 3 summarizes the results of the different types of design. This table also includes the total manufacturing costs and the comparison with the traditional design (D1).

A first evaluation of the results shows that material optimization seems to be more effective for this type of small-span element than geometric one. TH girders are a good option, with the additional advantage of not needing the extra construction effort required by tapered girders. The TLH girder option appears to be effective in these elements as the additional costs of the joints are not significant due to the low section depth offered by some solutions. Note how the seemingly most complete option (TLHVS girders) results in THVS elements, as the freedom to vary both material and geometry throughout the element is more than enough. Therefore, solutions use the same material in the plates longitudinally to avoid implementing additional joints. That is, instead of changing the material in the longitudinal direction (which introduces additional joints), the geometry is changed. The material is differentiated in the transverse plane, i.e., between flanges and the web.

D1, traditional design; *D2*, transverse geometric optimization; *D3*, transverse geometric and material optimization (TH girders); *D4*, transverse and longitudinal geometric optimization (HoVS girders); *D5*, transverse and longitudinal material optimization (TLH girders); *D6*, transverse material and transverse-longitudinal geometric optimization (THVS girders); *D7*, transverse-longitudinal geometric and material optimization (TLHVS girders).

Figure 5 summarizes graphically the main properties of the solutions obtained. It is evident how the typologies that change the geometrical properties along the length of the element tend to present more slender elements in the central section. In this case, it allows lower-quality steel and reduces material costs. It can also be seen how these solutions require less material in the flanges since they are further away from the centroid of the section, increasing their inertia and contribution to the section's resistant capacity. Another relevant aspect is the comparison between homogeneous and transversely hybrid tapered elements. The figure shows how increasing the steel quality in the flanges allows for obtaining less slender girders. It is also beneficial in reducing the weight of the structure. The other aspects are discussed in

Table 3 Optimal results of the different design approaches for the 6 m girder

Design				Geom. variables (mm)							Material configuration (f_{y_w}—f_{y_f}, MPa)				Cost (€)	Saving(%)†
				h_w 1*	h_w 2	h_w 3	h_w 4**	t_w	b_f	t_f	1 st *	2nd	3rd	Cent**		
D1				-	-	-	380	8	180	12	-	-	-	355–355	519	-
D2		Mat Cons		-	-	-	810	5	100	10	-	-	-	355–355	422	18.69
		Mat Var		-	-	-	900	5	120	10	-	-	-	275–275	417	19.65
D3				-	-	-	430	5	240	6	-	-	-	235–450	360	30.64
D4	Mat Cons		2TPs	290	-	-	900	5	100	8	-	-	-	355–355	402	22.54
			4TPs	140	600	-	860	5	110	8	-	-	-	355–355	400	22.93
			6TPs	120	500	770	900	5	100	8	-	-	-	355–355	399	23.12
	Mat Var		2TPs	350	-	-	1070	5	130	8	-	-	-	235–235	384	26.01
			4TPs	190	760	-	1100	5	100	10	-	-	-	235–235	382	26.40
			6TPs	140	590	950	1090	5	100	10	-	-	-	235–235	380	26.78
D5			2TPs	-	-	-	430	5	240	6	235–235	-	-	235–450	357	31.21
			4TPs	-	-	-	430	5	240	6	235–235	235–355	-	235–450	355	31.60
			6TPs	-	-	-	430	5	240	6	235–235	235–275	235–355	235–450	355	31.60
D6			2TPs	150	-	-	770	5	110	10	-	-	-	235–450	350	32.56
			4TPs	140	670	-	830	5	100	10	-	-	-	235–450	348	32.95
			6TPs	140	180	680	830	5	100	10	-	-	-	235–450	345	33.53
D7			2TPs	150	-	-	770	5	110	10	235–450	-	-	235–450	350	32.56
			4TPs	140	670	-	830	5	100	10	235–450	235–450	-	235–450	348	32.95
			6TPs	140	180	680	830	5	100	10	235–450	235–450	235–450	235–450	345	33.53

*Extreme configuration

**Central configuration

†Compared to the traditional design D1

the section where the main properties of each solution are summarized and compared as a function of the case study.

3.2 Girder of 14 m

For this case of greater length, the geometric component seems more important than the material. It can be seen how the designs that focus on varying the material (D3, D5) lose relevance concerning those that significantly influence the geometric component. D4 gives outstanding results, even when the fixed material is used. In this case, the TLHVS elements also find their optimal configuration in the THVS typology.

Table 4 and Fig. 6 show that, for this case, the D4 approach with the material as a variable in the optimization provides solutions with high-quality steel (S700). Therefore, the elements are less slender than those obtained using D6. However, it should be noted that this last approach allows the efficient use of lower-quality steels (transverse hybrid configuration), and the elements are designed with an aspect ratio similar to those obtained with D4. On the other hand, the elements with longitudinally variable cross-sections are more slender and have less material in the flanges than the others. It should also be noted that there are many coincidences in properties, such as taper angles, which will be discussed later.

3.3 Girder of 20 m

In this case, the geometrical component is even more decisive than the previous one. Therefore, regarding the behavior of the spectrum, it can be said that for elements of small spans, the material component is more significant. In contrast, as the span increases, a variable geometry in the longitudinal direction is more and more determinant. In Table 5, it can be seen how the D3 and D5 approaches lose relevance compared to those that vary the geometry longitudinally. Again, the TLHVS typology finds its optimal configuration in the THVS one.

Figure 7 shows a phenomenon similar to that of the 6 m element. It can be seen how the clever combination of different types of steel in flanges and webs makes the optimal THVS girder less slender than those obtained by D4. Another repeated aspect is the value of the taper angles and the zone where the transitions are made.

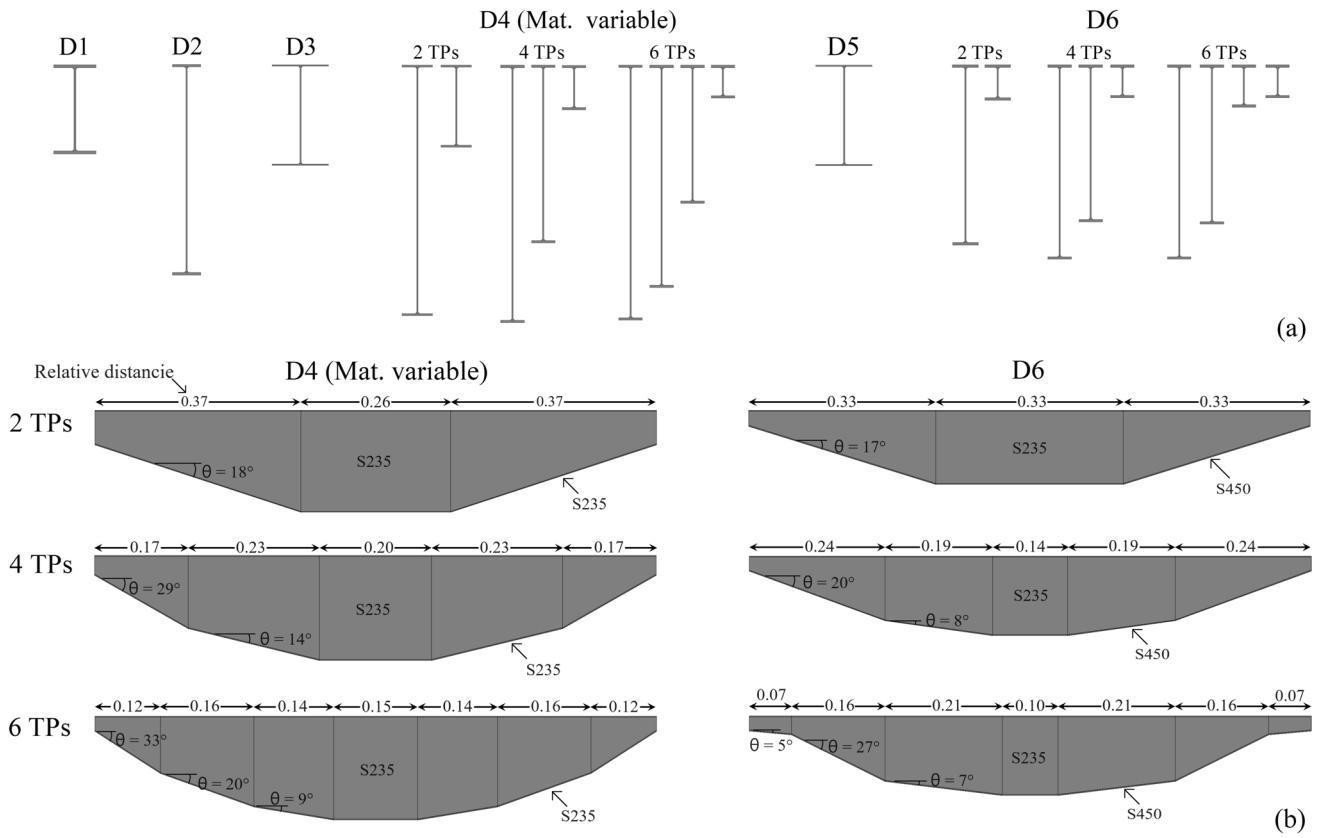

Fig. 5 Graphical representation of the most significant solutions for the 6 m girder. The vertical lines depicted on the web plate are shown to better identify where the transition is made, although for the designs shown no joints are required. θ: taper angle

3.4 Main properties of optimal configurations

This section summarizes and unifies criteria for determining common properties of the most efficient optimal configurations. These criteria serve as design recommendations for cases where optimization-assisted design is not implemented.

3.4.1 Savings

Firstly, the savings from using the different design approaches compared to the traditional one are summarized. Figure 8 highlights several aspects already mentioned. First, the design's efficiency based on optimizing the material for the case of $L=6$ m should be highlighted. In the other elements, the greater efficiency of the typologies with longitudinally variable cross-sections can be appreciated, as shown in the figure.

An exciting aspect is to compare the results of establishing hybrid construction over traditional homogeneous one. The differences are quite significant for the first case study, with an average saving of more than 10%. For case two, the difference drops to around 5%, while the differences oscillate around 2% for the last case. It reaffirms the previous comment on the importance of the geometrical component as the element span increases.

In general, the optimized designs show significant differences concerning the use of profiles. Note how the savings can reach almost 35% even for the first case. For the latter, the difference amounts to more than 60%. The use of profiles has many disadvantages, such as stiffness, since, in many cases, this criterion decides the design, especially in elements with large spans. Here, variable section girders are much more effective.

3.4.2 Span-to-depth ratio

The span-to-depth ratio is one of the most commonly used pre-sizing criteria for girders. Figure 9 shows the behavior of this indicator for all solutions. Note how many cases have more than one value due to tapered configurations. In general, common behaviors can be seen in many cases. The exception of the 6 m girder designed with the D6 approach and six transitions stands out. The graph

Table 4 Optimal results of the different design approaches for the 14 m girder

Design				Geom. variables (mm)							Material configuration (f_{y_w}—f_{y_f}, MPa)				Cost (€)	Saving (%)†
				h_w 1*	h_w 2	h_w 3	h_w 4**	t_w	b_f	t_f	1 st *	2nd	3rd	Cent**		
D1				-	-	-	650	15	350	25	-	-	-	355–355	2875	-
D2		Mat Cons		-	-	-	1770	5	210	15	-	-	-	355–355	1651	42.57
		Mat Var		-	-	-	1240	5	110	15	-	-	-	890–890	1547	46.19
D3				-	-	-	1130	5	570	5	-	-	-	355–700	1492	48.10
D4	Mat Cons		2TPs	450	-	-	1940	5	190	14	-	-	-	355–355	1438	49.98
			4TPs	240	1380	-	2000	5	180	14	-	-	-	355–355	1416	50.75
			6TPs	220	1110	1710	2000	5	180	14	-	-	-	355–355	1411	50.92
	Mat Var		2TPs	300	-	-	1420	5	150	12	-	-	-	700–700	1409	50.99
			4TPs	200	980	-	1420	5	150	12	-	-	-	700–700	1392	51.58
			6TPs	200	700	1080	1480	5	170	10	-	-	-	700–700	1388	51.72
D5			2TPs	-	-	-	1130	5	570	5	235–420	-	-	355–700	1458	49.29
			4TPs	-	-	-	1130	5	570	5	235–275	275–500	-	355–700	1448	49.63
			6TPs	-	-	-	1130	5	570	5	235–235	235–450	355–550	355–700	1437	50.01
D6			2TPs	310	-	-	1670	5	220	12	-	-	-	275–550	1317	54.19
			4TPs	220	1190	-	1630	5	190	12	-	-	-	355–600	1305	54.61
			6TPs	210	940	1360	1630	5	190	12	-	-	-	355–600	1302	54.71
D7			2TPs	310	-	-	1670	5	220	12	275–550	-	-	275–550	1317	54.19
			4TPs	220	1190	-	1630	5	190	12	355–600	355–600	-	355–600	1305	54.61
			6TPs	210	940	1360	1630	5	190	12	355–600	355–600	355–600	355–600	1302	54.71

*Extreme configuration

**Central configuration

†Compared to the traditional design D1. Design approaches (D's) are shown in Table 3

highlights the best solutions with thick lines. One aspect of relevance is this indicator's high values for the tapered girders' extreme sections. It is because, for the type of element studied, the predominant design constraint in the support zone is shear, which is solved with sections of low depth combined with high-strength steel.

The case taken as a reference is D6. In the previous section, it was discussed that hybrid configurations lose relevance for elements with large spans. However, in addition to the savings obtained with this approach, it should be remembered that less slender structures are obtained compared to D4. It means less weight, which is significant from the constructive point of view, for example, when transporting or manipulating the elements. In the case of $L = 6$ m, the optimum extreme sections are designed with a value of L/d ranging between 35 and 40. The second section (case with four or more transitions) is the exception for 6 TPs. In this case, the value is around 30. For 4 TPs, the value is around 8. The third (only appears in the cases with 6 TPs) and central sections have regular behaviors, with values between 6 and 8 in all cases.

For the 14 m case study, it can be seen that the extreme sections obtained with D4 are even less slender than those obtained with D6. Recall that optimal elements designed with high-strength steel are obtained with the D4 approach. In the case of D6, the extreme section for 2 TPs has an optimum L/d ratio of about 42. In the other two cases, the values range between 56 and 60. For the second section, the values are between 12 and 15. The value for the third section is around 10, while it drops to around 8–9 for the central one.

In the last case study, the values are also very stable. For the reference approach, the extreme value with two transitions increases compared to the previous cases to 50. For the other two configurations, the values are between 57 and 60. As in the previous case, the second section is between 10 and just over 15. The third section is also around 10, while the central ones coincide almost completely between 8 and 9.

3.4.3 Geometric flange-to-web ratio

According to an old rule, a rational I-section steel girder must have the same amount of steel in both flanges and the web. It means a geometric flange-to-web ratio (ρ_G), or ratio between the area of steel in both flanges and the web, equal to 1. This rule is for constant section (prismatic) elements. It has already been mentioned that optimum tapered girders have a slender central section with little material in the flanges, so this value should fall below 1. Figure 10 indeed

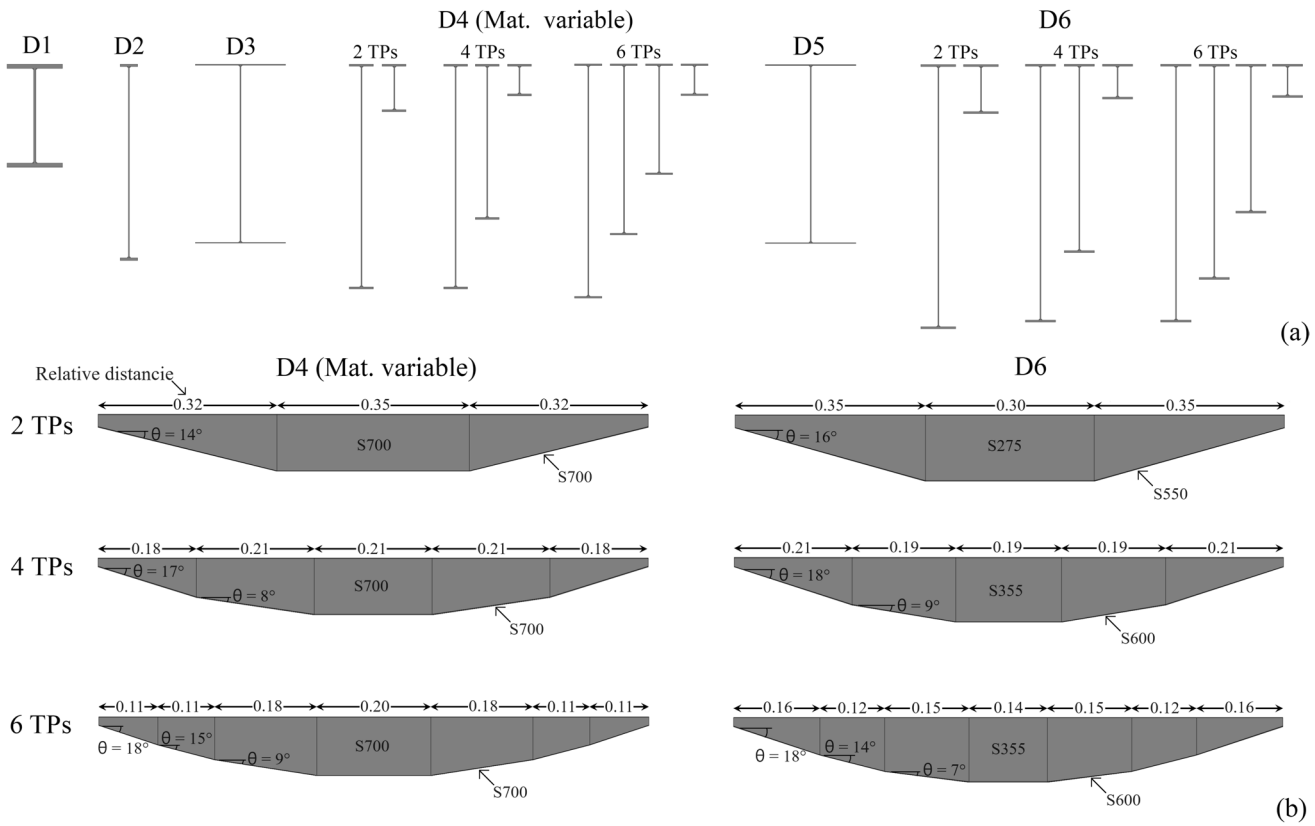

Fig. 6 Graphical representation of the most significant solutions for the 14 m girder. The vertical lines depicted on the web plate are shown to better identify where the transition is made, although for the designs shown no joints are required. θ: taper angle

shows that most central sections obtain their optimum configuration with a ρ_G value of about 0.5. That is, twice as much material regarding the flanges is on the web. The third section (closest to the central configuration) presents a slightly larger optimum value without reaching 1. The section in which the rule is fulfilled is the second one, while the one at the extremes reaches its optimum values (for D6) between 3 and 4, depending on the number of transitions in the element.

3.4.4 Taper angle and longitudinal configuration

Another helpful rule would be knowing the optimal taper angle for each configuration according to the number of transitions. Knowing the zone where these transitions should be established would also be of great interest. Table 6 shows the optimal taper angles for the three case studies with the two most effective variable section typologies. Here, there are quite clear trends, especially for the two larger elements.

For the case of where to set the transitions (see Figs. 5, 6, and 7), specific rules can also be deduced. Considering the three cases, the extreme configuration should measure about 34% of the total length for a homogeneous element of variable cross-section with two transitions. The extreme and second sections should have about 20% of the total length when four transitions are implemented. For 6, the extreme, second, and third portions should be 14, 13, and 15% of the total length. This configuration is pretty evenly distributed. Regarding transverse hybrid girders of variable cross-section, for two transitions, the rule remains the same as in the previous case: 34%. For four transitions, the distribution would be 23% and 19% for the extreme and second span, respectively. The result of the 6 m element is ignored for six transitions, and the other two are exactly the same: 16, 12, and 15% of the total length starting from the extreme configuration.

3.4.5 Optimum steel grades and hybrid ratios

Another recommendation of interest is related to the material component. Selecting the correct type of steel is essential for a rational design. In addition, there is the variant of selecting several types of steel for the same element. Remember that hybrid configurations help, in addition to reducing manufacturing cost to a greater or lesser extent, to reduce the weight compared to other optimal configurations.

For short-length elements, the most recommended steel is the lower quality (S235). Using S450 in the flanges

Table 5 Optimal results of the different design approaches for the 20 m girder

Design				Geom. variables (mm)							Material configuration (f_{y_w}—f_{y_f}, MPa)				Cost (€)	Saving(%)†
				h_w 1*	h_w 2	h_w 3	h_w 4**	t_w	b_f	t_f	1 st *	2nd	3rd	Cent**		
D1				-	-	-	930	20	450	35	-	-	-	355–355	7037	-
D2		Mat Cons		-	-	-	2480	5	270	18	-	-	-	355–355	3226	54.15
		Mat Var		-	-	-	1700	6	240	14	-	-	-	700–700	3175	54.88
D3				-	-	-	1920	6	260	16	-	-	-	355–600	3136	55.43
D4	Mat Cons		2TPs	770	-	-	2830	5	240	16	-	-	-	355–355	2763	60.74
			4TPs	760	2350	-	2830	5	240	16	-	-	-	355–355	2737	61.11
			6TPs	750	2150	2560	2680	5	260	16	-	-	-	355–355	2737	61.11
	Mat Var		2TPs	570	-	-	2530	5	230	16	-	-	-	420–420	2715	61.42
			4TPs	530	2130	-	2600	5	220	16	-	-	-	420–420	2675	61.99
			6TPs	510	1850	2380	2610	5	220	16	-	-	-	420–420	2670	62.06
D5			2TPs	-	-	-	1920	6	260	16	235–355	-	-	355–600	3028	56.97
			4TPs	-	-	-	1920	6	260	16	235–235	235–450	-	355–600	2971	57.78
			6TPs	-	-	-	1920	6	260	16	235–235	235–355	275–500	355–600	2967	57.84
D6			2TPs	370	-	-	2120	6	260	14	-	-	-	355–600	2676	61.97
			4TPs	320	1720	-	2120	6	260	14	-	-	-	355–600	2645	62.41
			6TPs	300	1260	1830	2180	6	220	16	-	-	-	355–600	2636	62.54
D7			2TPs	370	-	-	2120	6	260	14	355–600	-	-	355–600	2676	61.97
			4TPs	320	1720	-	2120	6	260	14	355–600	355–600	-	355–600	2645	62.41
			6TPs	300	1260	1830	2180	6	220	16	355–600	355–600	355–600	355–600	2636	62.54

*Extreme configuration

**Central configuration

†Compared to the traditional design D1. Design approaches (D's) are shown in Table 3

combined with S235 for the web is recommended to implement a hybrid transverse configuration. The case of $L = 14$ m is very curious, as high-quality steels tend to be used (e.g., S700). It is recommended to use S600 for the flanges and S355 for the web to implement hybrid configurations. In the latter case study, optimal homogeneous configurations tend to reduce the steel quality somewhat. The same as in the previous case is recommended to achieve a transverse hybrid configuration.

Table 7 summarizes the hybrid ratio values for the hybrid typologies. Note how, in general, the values are quite high, except for the extreme configurations for longitudinally hybrid elements. For girders with transverse hybridization, it is recommended to use values greater than 1.70.

3.5 Practical recommendations and applications

A guideline for the rational design of homogeneous or hybrid tapered steel girders is established based on the above recommendations. Following this methodology, a 25 m THVS element is designed, implementing two, four, and six transitions. The results are compared with those of a traditionally designed element. It consists of selecting the profile with the lowest weight that meets the established constraints. The general steps of the flow diagram in Fig. 11a and graphically represented in Fig. 11b are explained below, using the configuration with four transitions as an example. The final results are shown in this case, although the process required several iterations, as represented in the flowchart.

1. The first step is to analyze the problem. Aspects such as the span of the element, support conditions, type of loading, available steel grades, and so on, must be clarified.
2. Following the problem definition, the web is pre-sized. With the recommended L/d ratios, an initial value for h_w is proposed for the central section. It is important to note that this is an iterative process, as an estimate for the thickness of the flanges must be established to calculate h_w. In this case, the central section was initially set at a width of 2500 mm, with a thickness of 6 mm. However, the element did not meet several constraints, so a value of 8 mm was established. For the intermediate section (or second section as it is called in previous headings), a value of $h_w = 1800$ mm is set. The web's height of the extreme section is set to 450 mm.
3. Once the web is defined, it is proceeded to the flanges. Considering the central section's web, each flange is pre-sized so that the area of one flange is a quarter of the web (the two flanges should represent half of the web,

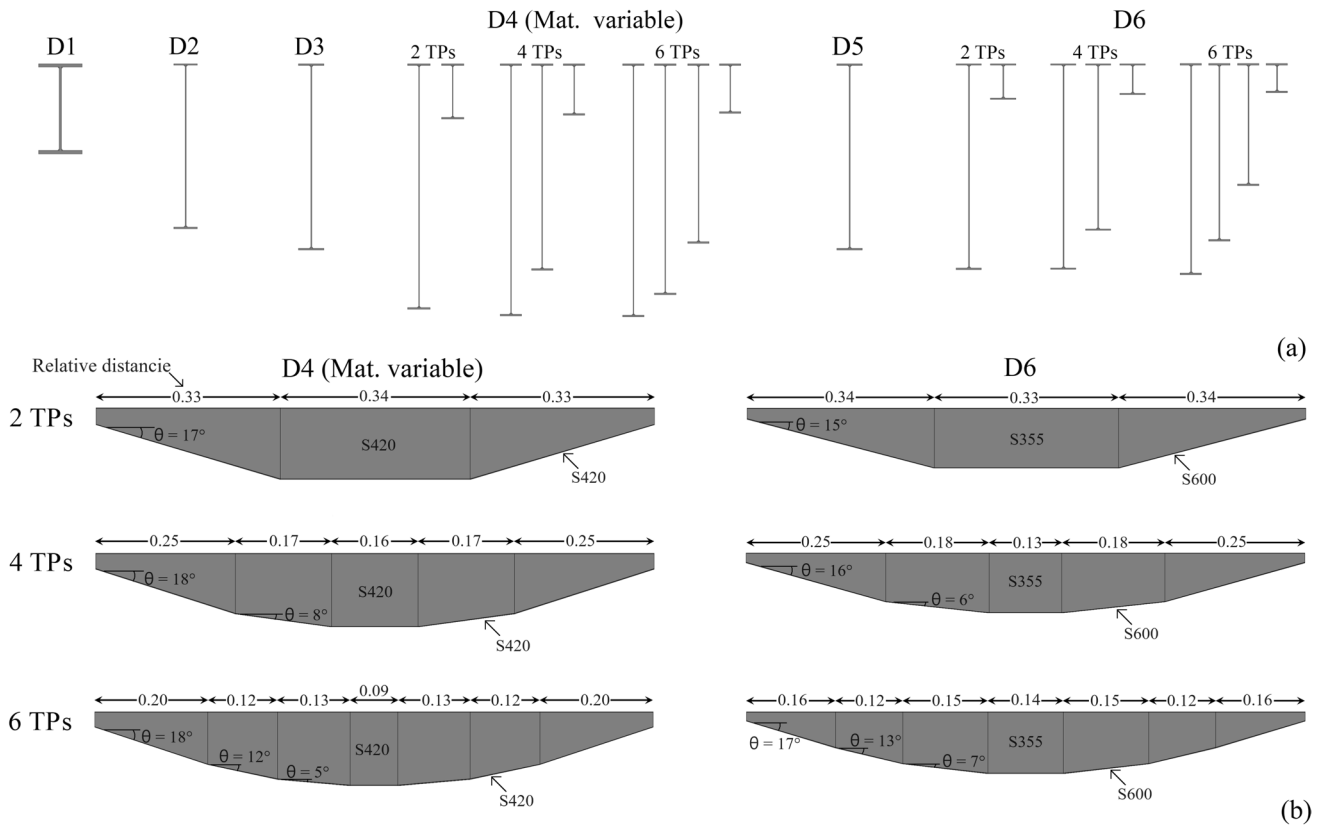

Fig. 7 Graphical representation of the most significant solutions for the 20 m girder. The vertical lines depicted on the web plate are shown to better identify where the transition is made, although for the designs shown no joints are required. θ: taper angle

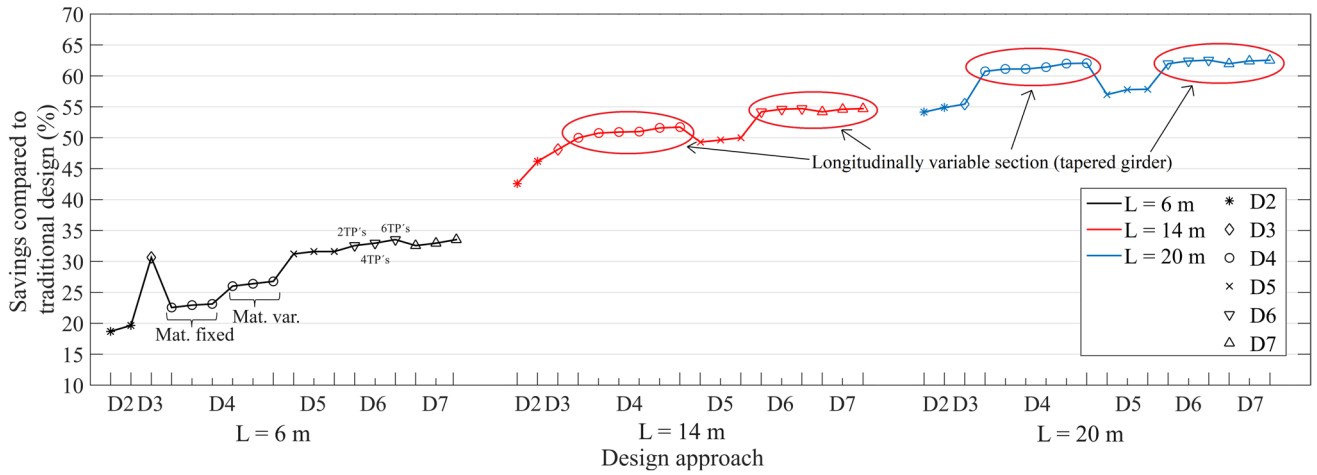

Fig. 8 Differences of optimization-based designs with respect to the traditional approach

which means a value of $\rho_G = 0.50$). In this case, establishing a thickness (t_f) of 14 mm represents a width (b_f) of 350 mm.

4. The results summarized in Sect. 3.4.4 are used to locate the transitions. This element would have a distribution of 5750 mm for the first span (extreme), 4750 for the second, and 4000 for the center. For the steel grades, it is decided to use S355 for the web and S600 for the flanges.
5. Once all the values are established, it is necessary to check the constraints. Those usually violated are bend-

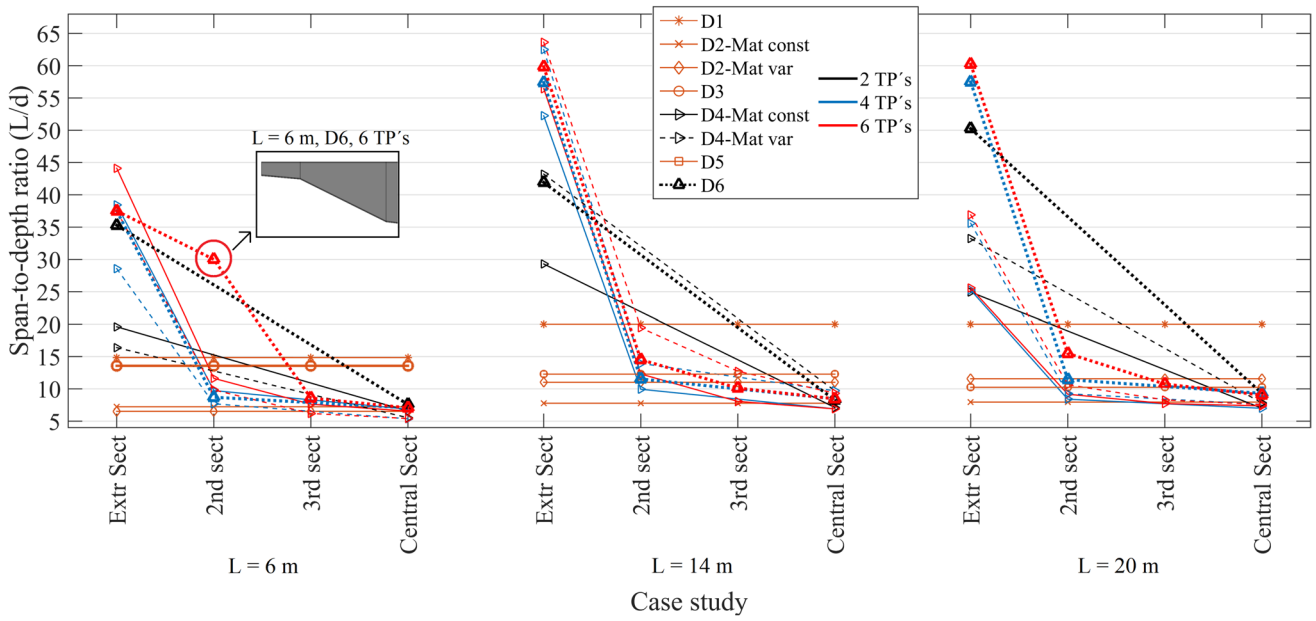

Fig. 9 Span-to-depth ratio for each case study based on each design approach

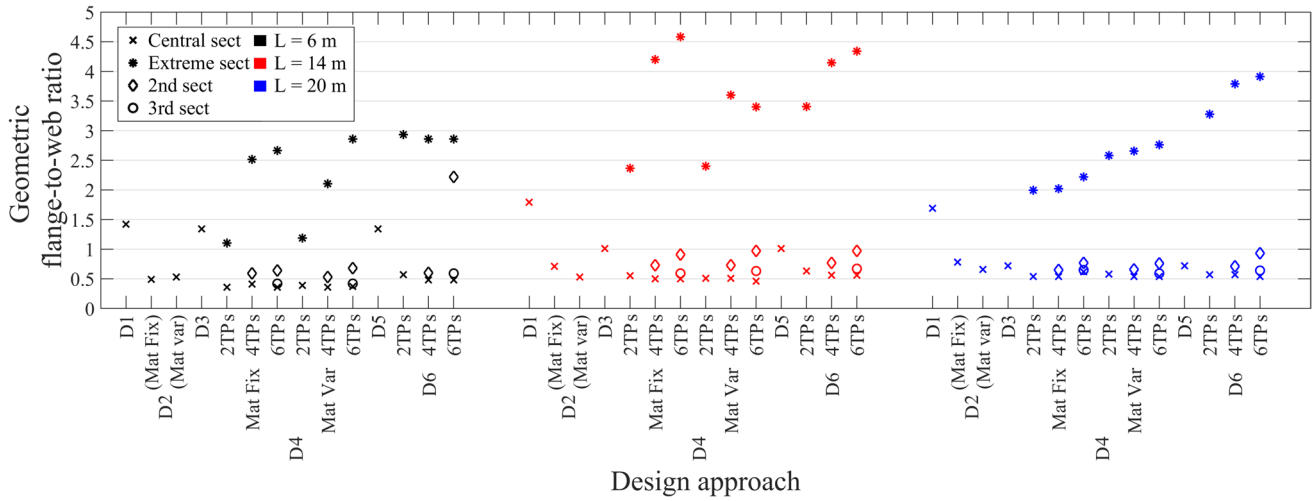

Fig. 10 Geometric flange-to-web ratios as a function of each design approach for the three cases

Table 6 Optimal taper angles for the three case studies implementing D4 (variable material) and D6

Case	Design	Optimal taper angle (°)					
		2 TPs	4 TPs		6 TPs		
		1st	1st	2nd	1st	2nd	3rd
$L=6$	D4 (Mat Var)	18	29	14	33	20	9
	D6	17	20	8	5	27	7
$L=14$	D4 (Mat Var)	14	17	8	18	15	9
	D6	16	18	9	18	14	7
$L=20$	D4 (Mat Var)	17	18	8	18	12	5
	D6	15	16	6	17	13	7

Table 7 Optimal R_h values for transverse and longitudinal hybrid elements

	$L=6$ m						$L=14$ m						$L=20$ m					
	D3	D5*				D6	D3	D5*				D6	D3	D5*				D6
		Extr	2nd	3rd	Cent			Extr	2nd	3rd	Cent			Extr	2nd	3rd	Cent	
Hybrid ratio	1.91	1.00	-	-	1.91	1.91	1.97	1.79	-	-	1.97	2.00	1.69	1.51	-	-	1.69	1.69
		1.00	1.51	-	1.91			1.17	1.82	-	1.97	1.69		1.00	1.91	-	1.69	
		1.00	1.17	1.51	1.91			1.00	1.91	1.55	1.97			1.00	1.51	1.82	1.69	

*Extr, 2nd, 3rd, and Cent are the four configurations starting from the extreme and ending with the central one. The three rows represent the typologies with 2, 4, and 6 TPs from top to bottom

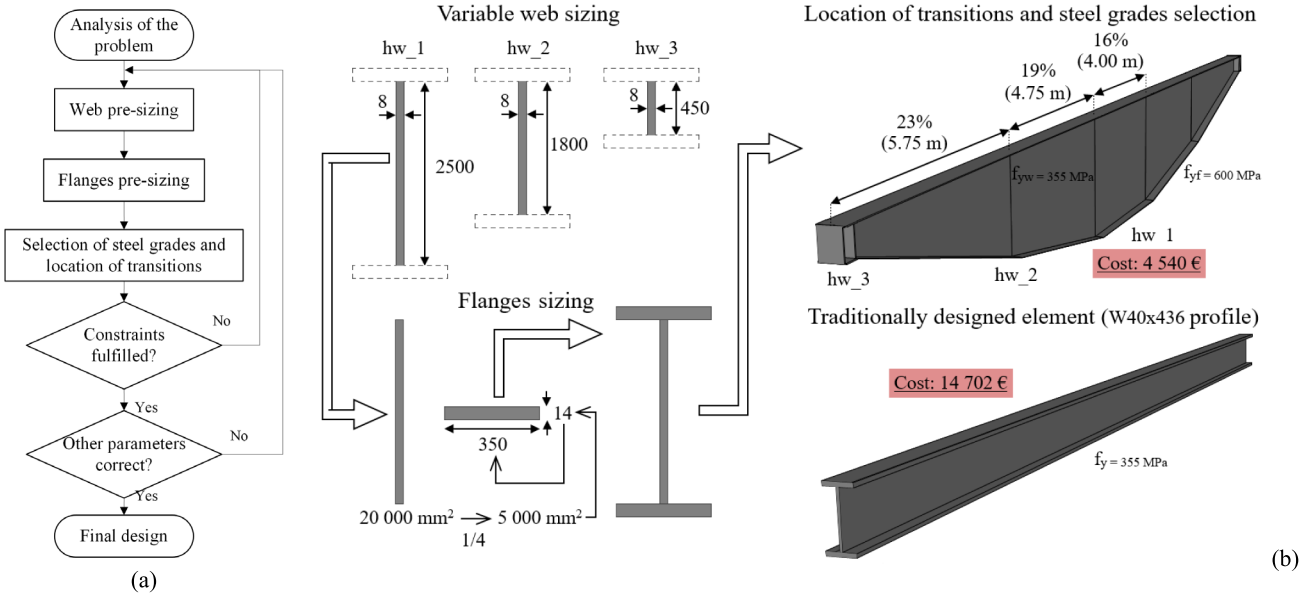

Fig. 11 **a** Flowchart of the design methodology based on the established recommendations; **b** graphical representation of the application of the proposed methodology. Cross-section dimensions are not to scale. 3D elements are to scale

ing resistance (especially in the center and adjacent sections), flange buckling against the web, and stiffness.

6. With all the constraints fulfilled, it is proceeded to analyze other parameters not used in the design, such as the taper angles. In this case, they are very close to the established values. For example, the value of θ of the extreme section is 13°. The recommended values are 20, 18, and 16° for 6, 14, and 20 m. Therefore, this trend suggests a decrease for the 25 m element, as it happens. Other values that can be checked are how far the constraints are from being violated. If it is too far away, the main parameters involved in that constraint should be identified and varied to make the difference as slight as possible.

It is necessary to emphasize that these recommendations are valid as a starting point for the design, and several modifications will indeed have to be made to achieve the most rational design possible. Table 8 and Fig. 11b show the results and their comparison with the selected profile (W40×436). Note that the original dimensions of the profile have been modified to match those formulated in the current problem.

This table demonstrates the superiority of THVS girders over traditional profiles. Note how the savings amount to more than 68%. Another interesting aspect is the difference between the THVS elements. Changing from two to four transitions improves the cost by 2.45% over the first typology. The improvement by setting six configurations is negligible. An optimization algorithm can probably further improve each design, and the difference by setting six transitions would be more significant.

Table 8 Representation of recommendation-assisted design and comparison with the traditional approach

Element		Geometric variables (mm)							Length of resulting spans (mm)				Mat config (f_{y_w}–f_{y_f}, Mpa)	Cost (€)	Saving(%)
		hw1*	hw2	hw3	hw4**	tw	bf	tf	1 st *	2nd	3rd	Central			
Prof. W40×436	-	-	-	-	930	35	415	60	-	-	-	25,000	355-355	14,702	-
THVS	2 TPs	500	-	-	2500	8	350	14	8500	-	-	8000	355-600	4654	68.34
-	4 TPs	450	1800	-	2500	8	350	14	5750	4750	-	4000	355-600	4540	69.12
-	6 TPs	400	1400	2000	2500	8	350	14	4000	3000	3750	3500	355-600	4520	69.26

*Extreme section

**Central section

†Represents the absolute distance, shown in Figs. 5, 6, and 7 as relative distance

4 Research limitations and future perspectives

This study has demonstrated more efficient alternatives to traditional construction methods. By allowing both geometry and material to vary freely in the optimization process, novel and cost-effective typologies, such as tapered hybrid girders (THVS girders), have been identified. However, despite these solutions' promising economic and structural benefits, significant challenges remain in advancing this field, and further research is required to address key limitations and practical implementation issues.

One of the main limitations of this study is the support conditions considered. While many structures use simply supported girders (e.g., bridges with isostatic spans, buildings with pinned beam-column connections), others require continuous support conditions, significantly altering the distribution of internal forces. Future research should extend beyond simply supported elements by modeling more complex structures, such as multi-span hyperstatic girders, or integrating the optimized girder into a complete structural system (e.g., a building or a steel box girder bridge). A similar issue arises with loading conditions, as optimizing the element within its actual structural context would allow for a more accurate assessment under realistic load states.

Another critical aspect requiring further investigation is the local behavior of the proposed typologies. While the economic indicators of THVS girders are significantly better than those of traditional designs, their unique geometries may introduce local weaknesses in certain areas. These potential failure mechanisms, such as local buckling or stress concentrations, must be evaluated through finite element analysis (FEA) and experimental testing on real specimens. It would enable the development of corrective measures, such as incorporating stiffeners as design variables in future optimization problems. Addressing these issues should be a key step toward updating design codes, which currently lack specific provisions for tapered or hybrid girders, particularly those that combine both factors.

A promising direction for further research is expanding the optimization criteria beyond cost minimization. While this study focused on welding, painting, sawing, and related manufacturing activities, future optimization frameworks should incorporate additional aspects such as structural performance (fire resistance, fatigue under dynamic loads), durability, and constructability. In particular, environmental considerations—including embodied carbon, material recycling potential, corrosion resistance, maintenance requirements, and life cycle performance—should be introduced into multi-objective optimization models. These factors should be analyzed holistically, considering the design and construction phase and long-term operational and end-of-life impacts, such as recycling potential and disposal costs.

Another key insight from this research is the potential application of THVS girders in small-span structures, such as buildings. Due to the high repetition of structural elements in building construction, even minor performance improvements at the element level can lead to significant overall benefits in terms of cost, weight, and material efficiency. Additionally, their lower weight compared to traditional reinforced concrete beams makes them an attractive alternative, as they reduce the demands on other load-bearing elements such as columns, load-bearing walls, and foundations. Thus, these novel typologies not only improve the sustainability of beam-type elements. The weight reduction also improves the overall environmental performance of the entire structural system by minimizing material consumption and construction impact. Figure 12 illustrates a potential application of THVS girders in a composite frame building structure, where their economic and environmental advantages can be combined with the high horizontal stiffness of RC columns to avoid the use of additional shear walls.

Despite these promising aspects, some practical challenges must be addressed before adopting THVS girders in the industry becomes widespread. One such challenge is material availability. The assumption that all steel grades are readily accessible may not hold true in certain regions, potentially affecting cost and feasibility. Future research

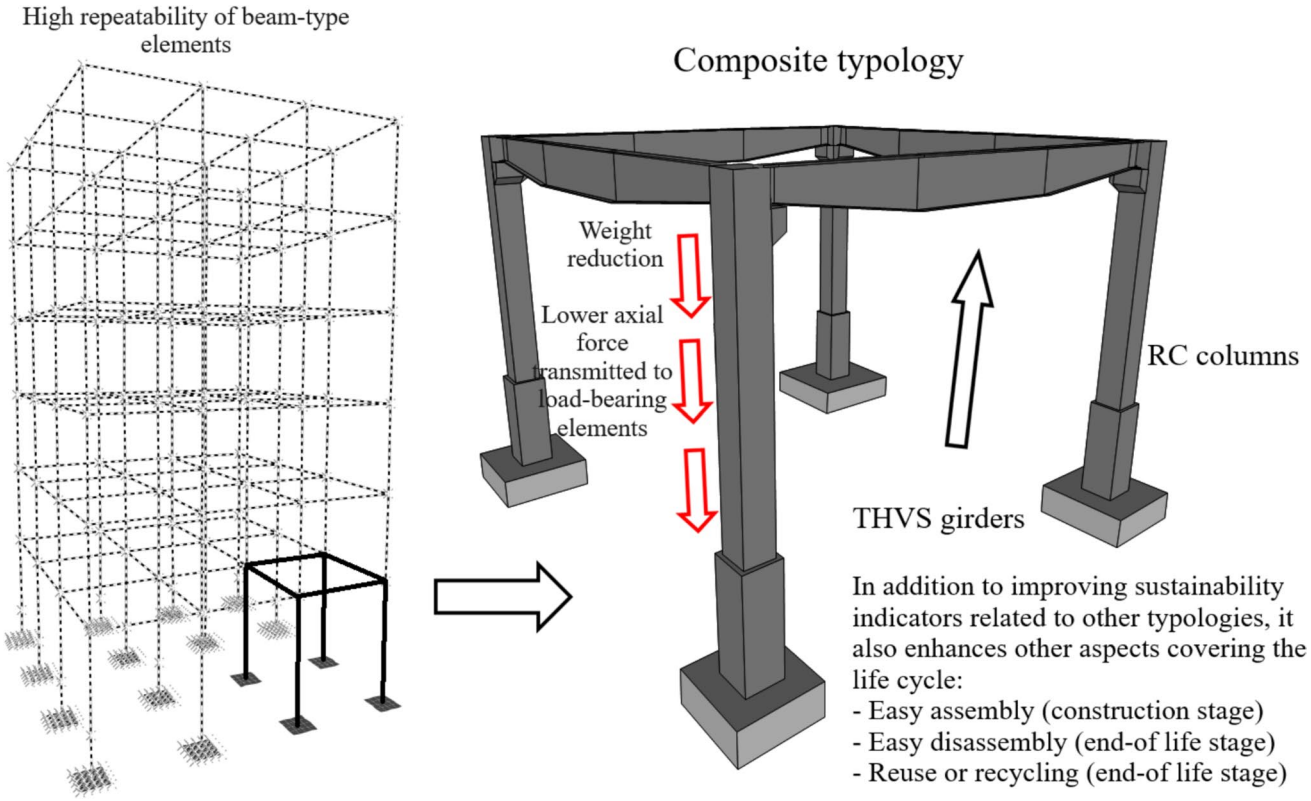

Fig. 12 Example of possible application of THVS girders

should explore the impact of regional material supply constraints on optimized designs and evaluate alternative solutions that balance performance and availability.

Another important consideration is the manufacturing complexity of tapered hybrid girders. While the optimization scheme proposed in this study shows significant theoretical economic advantages, the fabrication and construction of these elements (including precise welding of hybrid materials and handling variable cross-sections) may introduce technical and financial challenges. For instance, using different steel grades in flange and web plates may necessitate changes in welding wire, potentially increasing downtime during fabrication. Although such interruptions are implicitly considered through the inclusion of "non-productive time" in the cost estimation process, it is acknowledged that these values are empirical and may vary across different production settings. Moreover, while non-productive time has no direct environmental impact and is therefore excluded from environmental optimization models, it still introduces a degree of uncertainty into cost assessments.

In addition, the cutting of variable geometries, particularly in multi-tapered configurations, can result in steel plate waste. These potential losses are not currently modeled within the cost function. However, such offcuts could be reused (e.g., for stiffeners) or recycled, and even if their associated costs were included, the proposed hybrid tapered solutions would still offer significant economic/environmental advantages. Still, future optimization frameworks could be improved by incorporating explicit models for waste generation, handling, and reuse/recycling pathways, capturing not only the direct economic implications but also the environmental benefits. This would support a more holistic optimization strategy that aligns with emerging industry priorities toward circular steel use and low-carbon design.

Another important consideration for future studies is the impact of material sourcing and associated logistics. In specific scenarios, using different steel grades in hybrid girders may necessitate procurement from multiple suppliers, potentially introducing additional coordination requirements and transportation costs. While the current model captures transportation as a simplified cost component (based on the girder's weight or volume), this approach assumes consolidated sourcing and uniform delivery conditions. A more detailed, supply chain-aware framework that incorporates multi-source procurement, routing strategies, and logistics-related emissions could improve the accuracy of both economic and environmental assessments.

Finally, to maximize the real-world impact of this research, further efforts should focus on collaborating with

industry stakeholders to assess the feasibility of scaling up these optimized designs. A detailed cost–benefit analysis comparing traditional and optimized solutions in full-scale construction projects could provide valuable insights for both engineers and decision-makers. Bridging the gap between optimization research and practical implementation is essential to fully realize the potential of tapered hybrid girders in modern construction.

5 Concluding remarks

This study proposes an advanced optimization framework for the mechanical design of welded I-section steel plate girders, a structural element widely used in construction. By leveraging metaheuristic optimization techniques, the methodology enables simultaneous variation of geometry and material properties in both transverse and longitudinal planes, thereby enabling the development of high-performance girder typologies. Unlike conventional approaches focusing solely on minimizing weight or material cost, the objective function represents a comprehensive manufacturing cost, including key production activities such as welding, painting, or transportation. The design constraints comply with Eurocode 3 standards, ensuring structural reliability. Significantly, this framework enhances the efficiency and sustainability of structural design and directly informs manufacturing decision-making, offering tangible benefits to both the construction and steel fabrication industries. As such, the study contributes to the growing integration of design optimization, sustainable manufacturing, and construction engineering.

The results show that, for elements of shorter length, the material component is more significant than the geometry to obtain an optimal mechanical configuration. As the element span increases, the opposite happens and the geometry becomes more decisive. Of all the typologies analyzed, the most economical proved to be the transversely hybrid variable section (THVS) girder. This typology benefits from the longitudinal variation of the geometry and the transverse hybrid construction, so there is no need for additional longitudinal joints. The results allow the establishment of a design methodology based on the recommendations made. By applying this methodology to a different case study, a THVS element is designed to be almost 70% more economical than a girder (profile) selected by a traditional design approach.

Based on the limitations of this proposal, several lines of future research are open. One aspect of great relevance is the study of local phenomena that could affect the proposed typologies and, thus, provide possible alternatives (e.g., optimally positioned stiffeners). A further mandatory study should modify the support conditions by applying the proposed methodology to more complex elements (hyperstatic continuous girders, for example). Another alternative could be to insert them directly into the global structure (bridge, building) and optimize the whole system. An important aspect for future development involves refining the cost model to reflect real-world implementation better. Although the current model incorporates a wide range of manufacturing activities beyond material cost, future work could benefit from explicitly considering factors such as multi-supplier logistics, potential material waste, and reuse or recycling strategies. These additions would improve the realism of economic assessments and support the development of supply chain-aware and constructability-oriented optimization frameworks. Other exciting variants are based on improving the formulation. Implementing objective functions that measure environmental impact, structural performance (e.g., fire performance), durability, or constructability can provide more sustainable solutions. An additional aspect that could be decisive in the generalization of results is implementing the above criteria not only up to the design stage, but also focusing on life cycle analysis.

Author contributions I. N.: conceptualization, methodology, software, investigation, formal analysis, visualization, writing—original draft. M. K.: writing—review and editing, supervision, project administration. V. Y.: conceptualization, resources, supervision, project administration, writing—review and editing, funding acquisition.

Funding Open Access funding provided thanks to the CRUE-CSIC agreement with Springer Nature. This work was supported by the Grant PID2023-150003OB-I00, funded by MICIU/AEI/https://doi.org/10.13039/501100011033and by "ERDF/EU". Grant PRE2021-097197, funded by MICIU/AEI/https://doi.org/10.13039/501100011033and by FSE+. Grant CNPq 305484/2023–0, funded by the Brazilian National Council for Scientific and Technological Development.

Declarations

Conflict of interest The authors declare no competing interests.

References

1. Yong L, Zhifu M, Yuan X (2023) Towards advanced manufacturing systems for large parts: a review. Int J Adv Manuf Technol 125:3003–3022. https://doi.org/10.1007/s00170-023-10939-8
2. AbdelAleem BH, Ismail MK, Haggag M, El-Dakhakhni W, Hassan AAA (2022) Interpretable soft computing predictions of elastic shear buckling in tapered steel plate girders. Thin-Walled Struct 176:109313. https://doi.org/10.1016/j.tws.2022.109313
3. Ismail MK, AbdelAleem BH, Hassan AAA, El-Dakhakhni W (2023) Prediction of tapered steel plate girders shear strength using multigene genetic programming. Eng Struct 295:116806. https://doi.org/10.1016/j.engstruct.2023.116806
4. Sánchez-Garrido AJ, Navarro IJ, Yepes V (2022) Multi-criteria decision-making applied to the sustainability of building structures based on modern methods of construction. J Clean Prod 330:129724. https://doi.org/10.1016/j.jclepro.2021.129724
5. Terreros-Bedoya A, Negrin I, Payá-Zaforteza I, Yepes V (2023) Hybrid steel girders: review, advantages and new horizons in research and applications. J Constr Steel Res 207:107976. https://doi.org/10.1016/j.jcsr.2023.107976
6. Cucuzza R, Rosso MM, Marano GC (2021) Optimal preliminary design of variable section beams criterion. SN Appl Sci 3:745. https://doi.org/10.1007/s42452-021-04702-5
7. Vinot P, Cogan S, Piranda J (2001) Shape optimization of thin-walled beam-like structures. Thin-Walled Struct 39:611–630. https://doi.org/10.1016/S0263-8231(01)00024-6
8. Ozbasaran H, Yilmaz T (2018) Shape optimization of tapered I-beams with lateral-torsional buckling, deflection and stress constraints. J Constr Steel Res 143:119–130. https://doi.org/10.1016/j.jcsr.2017.12.022
9. Martins JP, Correia J, Ljubinković F, Simões da Silva L (2023) Cost optimisation of steel I-girder cross-sections using genetic algorithms. Structures 55:379–388. https://doi.org/10.1016/j.istruc.2023.06.030
10. Habashneh M, Cucuzza R, Domaneschi M, Rad MM (2024) Advanced elasto-plastic topology optimization of steel beams under elevated temperatures. Adv Eng Softw 190:103596. https://doi.org/10.1016/j.advengsoft.2024.103596
11. Kim Gh, Jeong K, Yoon J (2024) Optimum design of flattening process for roll-formed door impact beam with GPa-grade steel. Int J Adv Manuf Technol 134:2199–2215. https://doi.org/10.1007/s00170-024-14224-0
12. Hwang YM, Lin YQ, Cheng G (2025) Roller plunge schedule and roller design in straightening of metal H-beams. Int J Adv Manuf Technol 136:2245–2262. https://doi.org/10.1007/s00170-024-14942-5
13. Kaveh A, Kabir MZ, Bohlool M (2020) Optimum design of three-dimensional steel frames with prismatic and non-prismatic elements. Eng Comput 36:1011–1027. https://doi.org/10.1007/s00366-019-00746-9
14. Elhegazy H, Ebid A, AboulHaggag S, Mahdi I, AbdelRashid I (2023) Cost optimization of multi-story steel buildings during the conceptual design stage. Innov Infrastruct Solut 8:36. https://doi.org/10.1007/s41062-022-00999-2
15. Hlal F, Amani M, Al-Emrani M (2024) Stainless steel corrugated web girders for composite road bridges: optimization and parametric studies. Eng Struct 302:117366. https://doi.org/10.1016/j.engstruct.2023.117366
16. Chen D, Li F (2024) Intelligent construction design of high-rise steel structures based on multi-objective positioning algorithm and wireless sensor network. Int J Adv Manuf Technol. https://doi.org/10.1007/s00170-024-14809-9
17. Cucuzza R, Aloisio A, Rad MM, Domaneschi M (2024) Constructability-based design approach for steel structures: from truss beams to real-world inspired industrial buildings. Autom Constr 166:105630. https://doi.org/10.1016/j.autcon.2024.105630
18. Cucuzza R, Rad MM, Domaneschi M, Marano GC (2024) Sustainable and cost-effective optimal design of steel structures by minimizing cutting trim losses. Autom Constr 167:105724. https://doi.org/10.1016/j.autcon.2024.105724
19. Etaati B, Neshat M, Dehkordi AA, Pargoo NS, El-Abd M, Sadollah A, Gandomi AH (2024) Shape and sizing optimisation of space truss structures using a new cooperative coevolutionary-based algorithm. Results Eng 21:101859. https://doi.org/10.1016/j.rineng.2024.101859
20. Negrin I, Kripka M, Yepes V (2023) Design optimization of welded steel plate girders configured as a hybrid structure. J Constr Steel Res 211:108131. https://doi.org/10.1016/j.jcsr.2023.108131
21. Queguineur A, Daareyni A, Mokhtarian H et al (2025) Digital design and manufacturing of a railway bogie demonstrator via multi-material wire arc directed energy deposition. Int J Adv Manuf Technol. https://doi.org/10.1007/s00170-025-15132-7
22. Fielding DJ, Toprac AA (1967) Fatigue tests of hybrid plate girders under combined bending and shear [online]. Available at: https://library.ctr.utexas.edu/digitized/TexasArchive/phase1/96-2-CHR.pdf. Accessed Nov 2023
23. Carskaddan PS (1968) Shear buckling of unstiffened hybrid beams. J Struct Div 94:1965–1990. https://doi.org/10.1061/JSDEAG.0002039
24. Azizinamini A, Hash JB, Yakel AJ, Farimani R (2007) Shear capacity of hybrid plate girders. J Bridg Eng 12(5):535–543. https://doi.org/10.1061/(ASCE)1084-0702(2007)12:5(535)
25. Tran VL, Kim JK (2024) Hybrid machine learning models for classifying failure modes of unstiffened steel plate girders subjected to patch loading. Structures 59:105742. https://doi.org/10.1016/j.istruc.2023.105742
26. Shokouhian M, Shi Y (2015) Flexural strength of hybrid steel I-beams based on slenderness. Eng Struct 93:114–128. https://doi.org/10.1016/j.engstruct.2015.03.029
27. Wang C, Duan L, Frank Chen Y, Wang S (2016) Flexural behavior and ductility of hybrid high-performance steel I-girders. J Constr Steel Res 125:1–14. https://doi.org/10.1016/j.jcsr.2016.06.001
28. Zhu Y, Yun X, Gardner L (2023) Behaviour and design of high-strength steel homogeneous and hybrid welded I-section beams. Eng Struct 275:115275. https://doi.org/10.1016/j.engstruct.2022.115275
29. Zhang JW, Duan L, Wang CS, Wang YW (2024) Elastic-plastic flexural behavior of hybrid steel girder bridge considering welded residual stress. Struct Infrastruct Eng 1–23. https://doi.org/10.1080/15732479.2024.2332429
30. Luo Z, Shi Y, Xue X, Xu L (2024) Fire-resistance design of ultimate and serviceability limit states for Q690 high-strength steel plate girders under patch loading. Structures 59:105744. https://doi.org/10.1016/j.istruc.2023.105744
31. Bhat RA, Gupta LM (2021) Behaviour of hybrid steel beams with closely spaced web openings. Asian J Civ Eng 22:93–100. https://doi.org/10.1007/s42107-020-00300-9
32. Bock M, Gkantou M, Theofanous M, Afshan S, Yuan H (2023) Ultimate behaviour of hybrid stainless steel cross-sections. J Constr Steel Res 210:108081. https://doi.org/10.1016/j.jcsr.2023.108081
33. Mela K, Heinisuo M (2014) Weight and cost optimization of welded high-strength steel beams. Eng Struct 79:354–364. https://doi.org/10.1016/j.engstruct.2014.08.028
34. Skoglund O, Leander J, Karoumi R (2020) Optimizing the steel girders in a high-strength steel composite bridge. Eng Struct 221:110981. https://doi.org/10.1016/j.engstruct.2020.110981

35. Veljkovic M, Johansson B (2004) Design of hybrid steel girders. J Constr Steel Res 60:535–547. https://doi.org/10.1016/S0143-974X(03)00128-7
36. EN 1993–1–5 (2006) Eurocode 3: design of steel structures. Part 1–5: Plated structural elements. CEN. Available at: https://www.phd.eng.br/wp-content/uploads/2015/12/en.1993.1.5.2006.pdf. Accessed Nov 2023
37. Haapio J (2012) Feature-based costing method for skeletal steel structures based on the process approach. Ph.D. thesis, Tampere University of Technology. Available at: https://trepo.tuni.fi//handle/10024/114746. Accessed Nov 2023
38. EN 1993–1–1 (2005) Eurocode 3: design of steel structures. Part 1–1: General rules and rules for buildings. CEN. Available at: https://gaprojekt.com/wp-content/uploads/2021/11/Eurocode-3-Design-Of-Steel-Structures.pdf. Accessed Nov 2023
39. Negrin I, Kripka M, Yepes V (2023) Multi-criteria optimization for sustainability-based design of reinforced concrete frame buildings. J Clean Prod 425:139115. https://doi.org/10.1016/j.jclepro.2023.139115
40. Simon D (2008) Biogeography-based optimization. IEEE Trans Evol Comput 12(6):702–713. https://doi.org/10.1109/TEVC.2008.919004
41. Negrin I, Kripka M, Yepes V (2023) Metamodel-assisted meta-heuristic design optimization of reinforced concrete frame structures considering soil-structure interaction. Eng Struct. https://doi.org/10.1016/j.engstruct.2023.116657
42. Payá-Zaforteza I, Yepes V, González-Vidosa F, Hospitaler A (2010) On the Weibull cost estimation of building frames designed by simulated annealing. Meccanica 45:693–704. https://doi.org/10.1007/s11012-010-9285-0